

## Identification of New Functional Inhibitors of Acid Sphingomyelinase Using a Structure–Property–Activity Relation Model

Johannes Kornhuber,<sup>\*,†</sup> Philipp Tripal,<sup>†</sup> Martin Reichel,<sup>†</sup> Lothar Terfloth,<sup>‡</sup> Stefan Bleich,<sup>†</sup> Jens Wiltfang,<sup>†</sup> and Erich Gulbins<sup>‡</sup>

Department of Psychiatry and Psychotherapy, University of Erlangen, Germany, Molecular Networks, Erlangen, Germany, and Department of Molecular Biology, University of Duisburg–Essen, Germany

Received May 4, 2007

Some organic weak bases induce a detachment from inner lysosomal membranes and subsequent inactivation of acid sphingomyelinase (ASM) and thus work as functional ASM inhibitors. The aim of the present investigation was to develop a structure–property–activity relation (SPAR) model in order to specify the structural and physicochemical characteristics of probes capable of functionally inhibiting ASM. High  $pK_a$  and high  $\log P$  values are necessary but not sufficient preconditions for functional inhibition of ASM. The experimental data supported the requirement of an additional factor, which is necessary for functional inhibition of ASM. This factor  $k$  is related to the steric hindrance of the most basic nitrogen atom and presumably modulates the free presentation of a protonated nitrogen atom at the inner lysosomal surface. During the course of the study, we characterized 26 new functional ASM inhibitors, including doxepine **63**, fluoxetine **104**, maprotiline **109**, nortriptyline **114**, paroxetine **118**, sertraline **124**, suloctidil **125**, and terfenadine **127**.

### Introduction

Eukaryotic cells have the ability to internally segregate aqueous compartments differing in pH using lipid bilayer membranes and ATP-driven proton pumps.<sup>1–5</sup> The lysosomal membrane is usually much more permeable to the uncharged form of weak bases. However, inside of the lysosome, the bases become protonated and trapped, a phenomenon called lysosomotropism.<sup>3,6</sup> Many of the approved drugs for the treatment of human diseases contain basic functional groups that result in lysosomotropism. The accumulation of such drugs in acidic intracellular structures is partly responsible for their high apparent volume of distribution and high tissue concentrations.<sup>7–9</sup>

The acid sphingomyelinase (ASM<sup>a</sup>, EC 3.1.4.12, sphingomyelin phosphodiesterase, optimum pH 5.0) is an intralysosomal glycoprotein catalyzing the degradation of sphingomyelin to phosphorylcholine and ceramide. Ceramide induces apoptosis in many cells activated by proapoptotic receptors or stress stimuli.<sup>10,11</sup> Ceramide is further metabolized to sphingosine and sphingosine-1-phosphate. While the biological function of sphingosine is largely unknown, sphingosine-1-phosphate is involved in cellular differentiation, proliferation, and cell migration.<sup>12–16</sup> Since the 1970s, it has frequently been shown that weak organic bases have the potential to inhibit the activity of ASM.<sup>17–20</sup> It has been suggested that ASM is bound to intralysosomal membranes, thereby being protected against

inactivation. Weak bases such as desipramine (**17**) result in a detachment of the ASM from the inner membrane<sup>21</sup> and subsequent inactivation, possibly by proteolytic degradation.<sup>22</sup> Weak bases, therefore, do not directly inhibit ASM but result in a functional inhibition of ASM. According to this model, functional inhibition of ASM depends on high lysosomal concentrations of a weak basic drug (Figure 1).

Functional inhibition of ASM might be of major clinical relevance since ASM and its reaction products ceramide, sphingosine, and sphingosine-1-phosphate play a role in apoptosis, cellular differentiation, proliferation, infection, and cardiovascular disease (see Results and Discussion). Agents that reduce ASM activity and ceramide levels tend to attenuate apoptosis and promote cell proliferation,<sup>10,23</sup> possibly exhibit antidepressant effects in major depressive disorders,<sup>19,24</sup> and might exhibit beneficial clinical effects in acute or chronic neurodegenerative disorders such as stroke and Alzheimer's dementia.

The lack of a general model for weak basic drug-induced functional inhibition of ASM hinders a rational drug design of, or screening for, potential ASM-inhibitors. In an effort to overcome this, we have developed a structure–property–activity relation (SPAR) model, specifying the structural and physicochemical properties of drugs inducing functional inhibition of ASM. We identified a number of compounds which had previously been characterized as functional ASM inhibitors and used them as a first approach to estimate data on the physicochemical properties of functional ASM inhibitors. We then used a training set in order to define the structural and physicochemical preconditions for functional ASM inhibition and validated the SPAR model using another set of drugs. High  $pK_a$  and high  $\log P$  values are necessary but not sufficient preconditions for functional inhibition of ASM. A further factor is related to the steric hindrance of the most basic nitrogen atom. During the course of the studies, we identified 26 novel functional ASM inhibitors, most of them Food and Drug Administration (FDA)-approved known bioactive compounds, which are highly likely

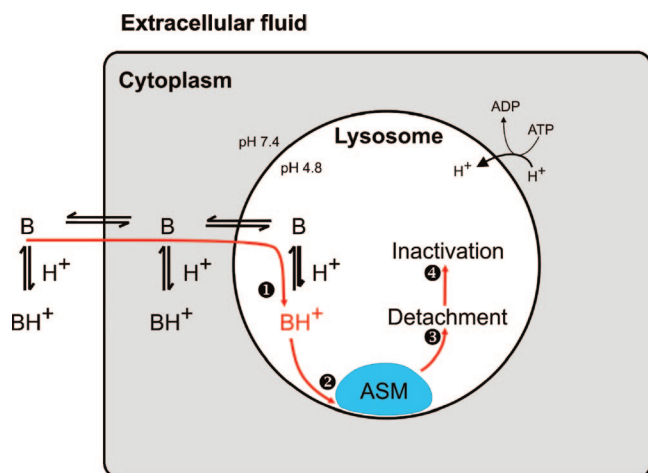
\* To whom correspondence should be addressed. Address: Johannes Kornhuber, M.D., Department of Psychiatry and Psychotherapy, University of Erlangen, Schwabachanlage 6, D-91054 Erlangen, Germany. Tel.: # 49-9131-853-4166. Fax.: #49-9131-853-4862. E-mail: Johannes.Kornhuber@uk-erlangen.de.

<sup>†</sup> Department of Psychiatry and Psychotherapy, University of Erlangen.

<sup>‡</sup> Molecular Networks, Erlangen.

<sup>‡</sup> University of Duisburg–Essen.

<sup>a</sup> Abbreviations: ASM, acid sphingomyelinase; AUC, area under the curve; BMP, bis(monoacylglycero)phosphate; FBS, fetal bovine serum; FDA, Food and Drug Administration; ROC, receiver operating characteristic; SPAR, structure–property–activity relationship; WHO, World Health Organization.



**Figure 1.** The figure shows a schematic model of how weak bases cumulate intralysosomally, thereby functionally inhibiting ASM. A low lysosomal pH is maintained by an ATP-driven proton pump. (1) Weak bases (B) cumulate in intracellular acidic compartments because the lysosomal membrane is much less permeable for the charged protonated bases (BH<sup>+</sup>) compared to the uncharged form, a phenomenon called lysosomotropism. Substances with high log *P* and high p*K*<sub>a</sub> values result in high intralysosomal concentrations. The enzyme acid sphingomyelinase (ASM) is attached by electrostatic forces to the inner lysosomal membrane, thereby being protected against proteolysis. ASM is active in the membrane-bound form and degrades sphingomyelin to phosphorylcholine and ceramide. (2) High concentrations of the protonated bases disturb the binding of ASM to the inner lysosomal membrane and result in a detachment of ASM (3) and subsequent inactivation (4), possibly involving proteolysis.<sup>21</sup> For further details, see the Introduction section.

to be minimally toxic and potentially rapidly available for clinical usage (amlodipine **41**, astemizole **43**, benztropine **45**, bepridil **46**, camylofin **50**, chlorprothixene **94**, clomiphen **55**, cloperastine **56**, cyclobenzaprine **59**, cyproheptadine **60**, doxepine **63**, drofenine **64**, fendiline **102**, fluoxetine **104**, maprotiline **109**, norfluoxetine **113**, nortriptyline **114**, paroxetine **118**, pimethixene **80**, promazine **84**, promethazine **120**, protriptyline **85**, sertraline **124**, sulotidil **125**, terfenadine **127**, and trifluorpromazine **129**).

## Results and Discussion

Detachment of ASM from intralysosomal membranes and subsequent proteolytic degradation probably requires high lysosomal concentrations of weak basic drugs. The aim of our investigation was to describe a SPAR model, namely, to express structural and physicochemical properties of probes numerically and to relate these values to functional inhibition of ASM. First, a limited number of physicochemical and structural parameters were selected for investigation. We then defined three sets of compounds to determine the characteristics of functional ASM inhibitors, namely, a set selected from literature data, a training set, and a validation set.

**Selection of Physicochemical Parameters.** The pH partition theory<sup>3,6</sup> predicts that the lysosomal cumulation of weak bases increases between p*K*<sub>a</sub> values of approximately 6 and 8.5, when taking the intralysosomal pH as 4.8 and the cytoplasmic pH as 7.4. A comparable result was obtained experimentally with a series of substances with differing p*K*<sub>a</sub> values but otherwise similar physicochemical properties.<sup>25</sup> Diacidic bases result in dramatically increased accumulation ratios compared to those of monoacidic bases.<sup>5</sup> Furthermore, higher cumulation of weak basic drugs in lysosomes is related to the lipophilicity of the compound.<sup>26,27</sup> We concluded that potent drug-related variables

for the absolute lysosomal concentration of a weak basic drug are the p*K*<sub>a</sub> and log *P* values.

**Selection of Structural Parameters.** Which factor or factors might determine whether or not a compound with high p*K*<sub>a</sub> and high log *P* values acts as a functional ASM inhibitor? One approach to find such factors is to closely analyze the predicted ASM-inactivation mechanism (Figure 1) and the interaction of the ASM molecule at the inner leaf of the lysosomal membrane.<sup>21</sup> This inner leaf has a special lipid composition that is different from other cellular membranes, namely, a high concentration of bis(monoacylglycero)phosphate (BMP).<sup>28,29</sup> BMP was shown to remain negatively charged even at pH 4.2.<sup>30</sup> ASM has an isoelectric point of 6.8 and therefore possesses positively charged regions at intralysosomal pH values. These regions most likely contribute to the electrostatic interaction of the enzyme with the anionic membrane-bound lipid BMP.<sup>21</sup> The binding of ASM to lysosomal membranes is high in the presence of BMP,<sup>31</sup> and therefore, the negatively charged lysosomal lipids drastically stimulate the hydrolysis of membrane-bound sphingomyelin by ASM.<sup>31</sup> Lysosomotropic xenobiotic compounds, such as desipramine **17**, are supposed to partition into the inner leaf of the lysosomal membrane in such a way that the most lipophilic substituent at the cationic nitrogen atom is embedded between the lipid acyl chains, while the positively charged nitrogen atom is in the neighborhood of the negatively charged lipid head groups directed toward the inner surface of the lysosome. Cationic xenobiotic compounds thereby result in a detachment of ASM from the membrane and subsequent proteolytic inactivation by altering the surface charge and disturbing the electrostatic binding of ASM to the inner lysosomal membrane. This model allows the definition of one prerequisite for functional inhibition of ASM, namely, the sterically free presentation of a compound's cationic nitrogen atom at the inner surface of the lysosomal membrane. According to this model, we defined a new molecular descriptor (*k*) that predicts the steric hindrance of the cationic nitrogen atom. This descriptor *k* is defined as the sum of heavy atoms at the two smaller substituents at the most basic nitrogen atom. The largest substituent at the cationic nitrogen atom is assumed to partition into the inner leaf of the lysosomal membrane and therefore does not contribute to the steric hindrance of the cationic nitrogen atom. The counting algorithm for *k* is further detailed in the Experimental Section, including special situations that occur if the most basic nitrogen atom is part of a ring.

**Set Selected from Literature Data.** The literature search identified a series of exogenous substances (the "literature set") compounds **1–38**, Table 1, Figure 2) that had been tested for their effect on ASM activity.<sup>17–22,32–39</sup> Experimental data of this set do not allow the construction of a SPAR model but serve as a first impression since they are based on different experimental conditions (such as drug concentrations or incubations time) and different experimental models (such as PC12 cells or fibroblasts). Most compounds in the literature set were tested for inhibition of ASM at concentrations ranging from 5 to 50 μM. Compounds rated as functional ASM-inhibitors resulted in 50–90% inhibition of ASM activity. Figure 2 shows the position of the compounds in this set within the p*K*<sub>a</sub>–log *P* parameter space. It is noteworthy that all presently identified functional ASM inhibitors, which were discovered by chance and not via a hypothesis-driven systematic approach, segregate in a narrow area in the p*K*<sub>a</sub>–log *P* parameter space. It is evident that all previously identified functional ASM inhibitors have high p*K*<sub>a</sub> values (≥8.1) and high log *P* values (≥2.3). However, some compounds with high p*K*<sub>a</sub> and log *P* values did not inhibit

Table 1. Literature Set<sup>c</sup>

No	Structure	Generic name or substance code	no	Structure	Generic name or substance code
1		2-Hydroxy-imipramine $pK_a = 9.48^a$ $\log P = 4.06^a$ $k = 2$	2		6-Hydroxy-dopamine $pK_a = 10.3^{98}$ $\log P = -0.70^a$ $k = 0$
3		10-Hydroxy-imipramine $pK_a = 9.49^a$ $\log P = 3.14^a$ $k = 2$	4		Alimemazine $pK_a = 9.11^{99}$ $\log P = 4.81^{99}$ $k = 2$
5		Amiodarone $pK_a = 8.73^{64}$ $\log P = 7.57^b$ $k = 4$	6		Amitriptyline $pK_a = 9.40^{61}$ $\log P = 5.04^{59}$ $k = 2$ $ra = 11.7\%$
7		AY9944 $pK_a = 9.13^a$ $\log P = 6.02^a$ $k = 8$	8		Azacytidine $pK_a = 3.28^a$ $\log P = -2.17^{59}$ $k = 6$
9		Carbamazepine $pK_a = -0.49^a$ $\log P = 2.45^{59}$ $k = 0$	10		Chloroquine $pK_a = 9.94^{62}$ $\log P = 4.63^{59}$ $k = 4$
11		Chlorpromazine $pK_a = 9.30^{61}$ $\log P = 5.19^{59}$ $k = 2$ $ra = 42.4\%$	12		Clomipramine $pK_a = 9.38^{64}$ $\log P = 5.19^{59}$ $k = 2$
13		Cocaine $pK_a = 8.70^{64}$ $\log P = 2.30^{59}$ $k = 1$	14		Colcemide $pK_a = 8.48^a$ $\log P = 1.37^{100}$ $k = 1$
15		Cyamemazine $pK_a = 9.31^a$ $\log P = 4.62^a$ $k = 2$	16		Cycloheximide $pK_a = -4.79^a$ $\log P = 0.55^{59}$ $k = 0$

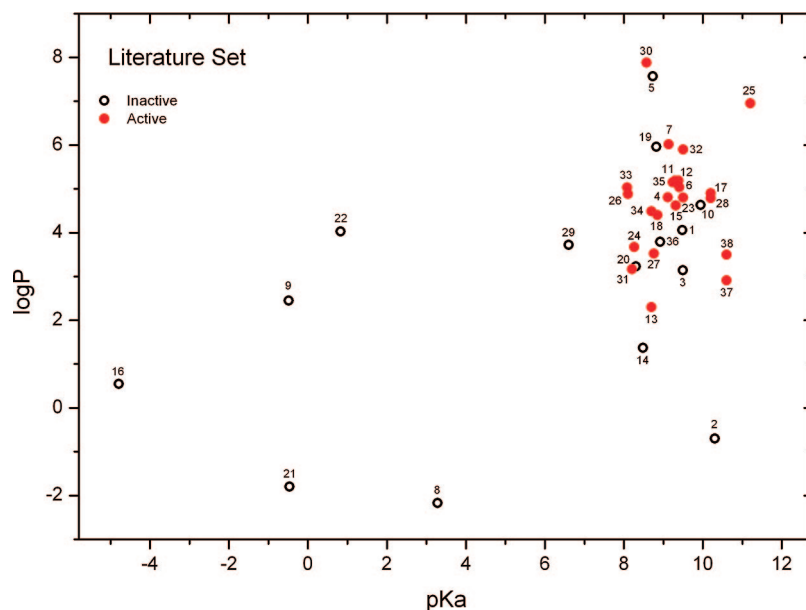
Table 1. (Continued)

No	Structure	Generic name or substance code	no	Structure	Generic name or substance code
17		Desipramine $pK_a = 10.20^{61}$ $\log P = 4.90^{59}$ $k = 1$	18		Dibucaine $pK_a = 8.85^{101}$ $\log P = 4.40^{59}$ $k = 4$
19		Fantofarone $pK_a = 8.82^a$ $\log P = 5.96^a$ $k = 13$	20		Haloperidol $pK_a = 8.30^{61}$ $\log P = 3.23^{59}$ $k = 12$ ra = 86.1%
21		Hydroxyurea $pK_a = -0.47^a$ $\log P = -1.80^{59}$ $k = 0$	22		Imidodibenzyle $pK_a = 0.83^a$ $\log P = 4.03^a$ $k = 0$
23		Imipramine $pK_a = 9.50^{61}$ $\log P = 4.80^{59}$ $k = 2$	24		Mianserin $pK_a = 8.26^a$ $\log P = 3.67^a$ $k = 1$
25		Perhexiline $pK_a = 11.20^a$ $\log P = 6.95^a$ $k = 0$ ra = 8.5%	26		Prochlorperazine $pK_a = 8.10^{61}$ $\log P = 4.88^{59}$ $k = 1$
27		Propericiacine $pK_a = 8.76^{102}$ $\log P = 3.52^{59}$ $k = 6$	28		Quinacrine $pK_a = 10.20^{62}$ $\log P = 4.79^a$ $k = 4$
29		Reserpine $pK_a = 6.60^{62}$ $\log P = 3.72^{103}$ $k = 6$	30		Tamoxifen $pK_a = 8.57^{104}$ $\log P = 7.88^a$ $k = 2$
31		Thioproperazine $pK_a = 8.21^a$ $\log P = 3.17^a$ $k = 1$	32		Thioridazin $pK_a = 9.50^{61}$ $\log P = 5.90^{59}$ $k = 1$ ra = 34.8%

Table 1. (Continued)

No	Structure	Generic name or substance code	no	Structure	Generic name or substance code
33		Trifluoperazin $pK_a = 8.08^{105}$ $\log P = 5.03^{59}$ $k = 1$	34		Trihexyphenidyl $pK_a = 8.70^{68}$ $\log P = 4.49^{59}$ $k = 5$ $ra = 83.9\%$
35		Trimipramine $pK_a = 9.24^{64}$ $\log P = 5.15^a$ $k = 2$ $ra = 13.8$	36		Verapamil $pK_a = 8.92^{64}$ $\log P = 3.79^{59}$ $k = 13$
37		W-5 $pK_a = 10.60^a$ $\log P = 2.91^a$ $k = 0$	38		W-7 $pK_a = 10.60^a$ $\log P = 3.50^a$ $k = 0$

<sup>a</sup> Calculated value from the ACD/LogD Suite (program version 10.02, Toronto, Canada).<sup>75</sup> <sup>b</sup> Experimental data cited in the internal database of the ACD program. <sup>c</sup> In the case of two or more nitrogen atoms, the most basic nitrogen, as determined by the ACD/LogD Suite, is marked by an asterisk. The number of heavy atoms at the strongest basic nitrogen atom ( $k$ ) is counted according to an algorithm described in the Experimental Section. Eight compounds from the literature set (amitriptyline **6**, chlorpromazine **11**, clomipramine **12**, haloperidol **20**, perhexiline **25**, thioridazin **32**, trihexyphenidyl **34**, trimipramine **35**) are also part of the validation set. Their experimental values  $ra$  [residual ASM activity, compared to control conditions (=100%)] are indicated.



**Figure 2.** A  $pK_a$ – $\log P$  property–activity diagram showing the distribution of the substances in the literature set in the parameter space. We identified 38 substances for which functional inhibition of ASM had previously been investigated<sup>17–22,32–39</sup> and that were available on the PubChem site (Table 1, substances **1–38**). Inhibition of ASM by more than 50% was rated positive. For further details, see the Experimental Section.

ASM (e.g., **5**, **10**, **19**; Figure 2). Imipramine **23** and its metabolites 2-hydroxy-imipramine **1** and 10-hydroxy-imipramine **3** are structurally related. In contrast to the parent substances, the metabolites are less lipophilic and did not functionally inhibit ASM.

**Training Set.** We selected 52 compounds with  $pK_a \geq 4.50$  and  $\log P \geq 2.26$  as a training set (Table 2, Figure 3A). None of these compounds had previously been tested as functional ASM inhibitors. Fourteen of the substances (amlodipine **41**, astemizole **43**, benzotropine **45**, bepridil **46**, camylofin **50**,

**Table 2.** Training Set<sup>c</sup>

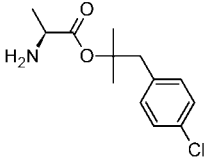
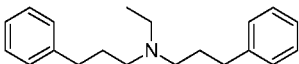
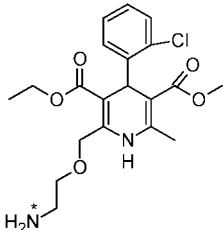
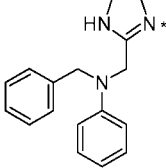
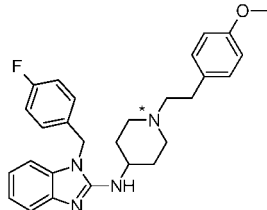
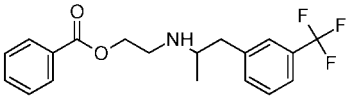
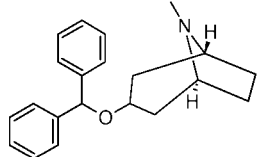
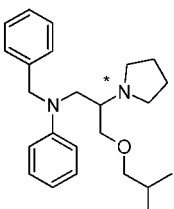
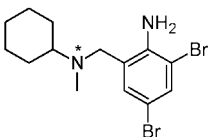
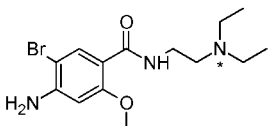
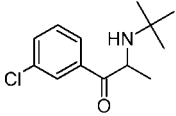
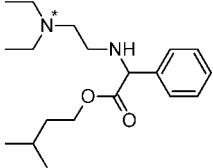
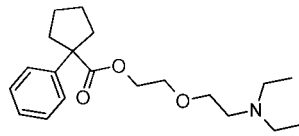
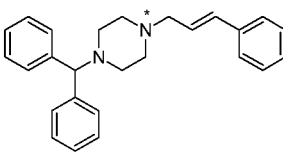
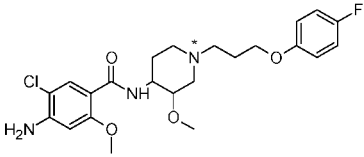
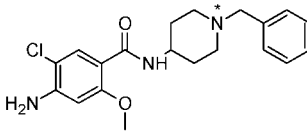
no	Structure	Generic name or substance code	no	Structure	Generic name or substance code
39		Alaproclate $pK_a = 7.76^a$ $\log P = 2.93^a$ $k = 0$ $ra = 92.3\%$	40		Alverine $pK_a = 9.51^a$ $\log P = 5.93^a$ $k = 11$ $ra = 61.9\%$
41		Amlodipine $pK_a = 8.60^{65}$ $\log P = 3.00^{65}$ $k = 0$ $ra = 12.0\%$	42		Antazoline $pK_a = 10.10^{74}$ $\log P = 4.24^{74}$ $k = 6$ $ra = 100.9\%$
43		Astemizole $pK_a = 8.50^{66}$ $\log P = 5.48^{66}$ $k = 10$ $ra = 49.8\%$	44		Benfluorex $pK_a = 8.59^a$ $\log P = 4.80^a$ $k = 11$ $ra = 100.4\%$
45		Benztropine $pK_a = 10.00^{63}$ $\log P = 3.75^{106}$ $k = 1$ $ra = 12.7\%$	46		Bepridil $pK_a = 9.21^a$ $\log P = 5.80^a$ $k = 4$ $ra = 34.5\%$
47		Bromhexine $pK_a = 8.50^{107}$ $\log P = 5.08^a$ $k = 7$ $ra = 106.8\%$	48		Bromopride $pK_a = 9.35^{108}$ $\log P = 2.83^{59}$ $k = 4$ $ra = 90.5\%$
49		Bupropion $pK_a = 7.16^a$ $\log P = 3.47^a$ $k = 4$ $ra = 117.9\%$	50		Camylofin $pK_a = 10.02^a$ $\log P = 5.57^a$ $k = 4$ $ra = 30.9\%$
51		Carbetapentane $pK_a = 9.69^a$ $\log P = 3.29^a$ $k = 4$ $ra = 88.7\%$	52		Cinnarizine $pK_a = 7.47^{109}$ $\log P = 5.77^{109}$ $k = 9$ $ra = 119.6\%$
53		Cisapride $pK_a = 7.90^{66}$ $\log P = 3.12^a$ $k = 11$ $ra = 101.3\%$	54		Clebopride $pK_a = 8.59^{108}$ $\log P = 2.72^{110}$ $k = 7$ $ra = 102.0\%$



Table 2. (Continued)

no	Structure	Generic name or substance code	no	Structure	Generic name or substance code
55		Clomiphene $pK_a = 9.60^a$ $\log P = 8.01^a$ $k = 4$ $ra = 13.0\%$	56		Cloperastine $pK_a = 8.87^a$ $\log P = 5.16^a$ $k = 5$ $ra = 40.5\%$
57		Cloricromen $pK_a = 9.86^a$ $\log P = 4.20^a$ $k = 4$ $ra = 119.5\%$	58		Cyclazocine $pK_a = 9.38^{111}$ $\log P = 3.31^{72}$ $k = 4$ $ra = 123.3\%$
59		Cyclobenzaprine $pK_a = 9.15^a$ $\log P = 5.00^a$ $k = 2$ $ra = 26.2\%$	60		Cyproheptadine $pK_a = 8.87^{112}$ $\log P = 4.69^{59}$ $k = 1$ $ra = 22.2\%$
61		Dilazep $pK_a = 8.29^a$ $\log P = 4.28^a$ $k = 18$ $ra = 102.3\%$	62		Domperidone $pK_a = 8.06^{108}$ $\log P = 4.05^{59}$ $k = 13$ $ra = 120.4\%$
63		Doxepine $pK_a = 9.00^{67}$ $\log P = 4.01^{67}$ $k = 2$ $ra = 46.6\%$	64		Drofenine $pK_a = 9.21^a$ $\log P = 5.59^a$ $k = 4$ $ra = 48.2\%$
65		Etomidate $pK_a = 4.50^{65}$ $\log P = 3.05^{59}$ $k = 6$ $ra = 109.1\%$	66		Fipexide $pK_a = 5.38^a$ $\log P = 3.05^a$ $k = 10$ $ra = 121.3\%$
67		Flunarizine $pK_a = 7.71^{109}$ $\log P = 6.42^{74}$ $k = 9$ $ra = 95.1\%$	68		Fluspirilene $pK_a = 8.66^{113}$ $\log P = 5.83^{113}$ $k = 16$ $ra = 103.9\%$
69		Harmine $pK_a = 7.50^{114}$ $\log P = 3.56^{59}$ $k = 6$ $ra = 92.1\%$	70		Lidocaine $pK_a = 7.94^{64}$ $\log P = 2.26^{59}$ $k = 4$ $ra = 123.9\%$

Table 2. (Continued)

no	Structure	Generic name or substance code	no	Structure	Generic name or substance code
71		Lofepamine $pK_a = 6.52^a$ $\log P = 6.96^a$ $k = 11$ $ra = 90.5\%$	72		Loratadine $pK_a = 4.58^{115}$ $\log P = 5.20^{59}$ $k = 6$ $ra = 118.3\%$
73		Mecamylamine $pK_a = 11.20^{62}$ $\log P = 3.06^a$ $k = 1$ $ra = 112.1\%$	74		Mibefradil $pK_a = 9.26^a$ $\log P = 3.86^{65}$ $k = 13$ $ra = 56.4\%$
75		Mifepristone $pK_a = 5.49^a$ $\log P = 4.95^a$ $k = 2$ $ra = 101.9\%$	76		Noscapine $pK_a = 6.20^{62}$ $\log P = 2.83^a$ $k = 1$ $ra = 114.8\%$
77		Oxybutynin $pK_a = 8.24^a$ $\log P = 5.19^a$ $k = 4$ $ra = 94.2\%$	78		Papaverine $pK_a = 6.25^{104}$ $\log P = 2.93^{116}$ $k = 6$ $ra = 118.2\%$
79		Penfluridol $pK_a = 8.40^a$ $\log P = 6.01^a$ $k = 17$ $ra = 79.9\%$	80		Pimethixene $pK_a = 8.83^a$ $\log P = 6.85^a$ $k = 1$ $ra = 32.0\%$
81		Pimozide $pK_a = 8.63^{113}$ $\log P = 6.30^{59}$ $k = 15$ $ra = 96.2\%$	82		Pridinol $pK_a = 9.71^a$ $\log P = 3.84^a$ $k = 5$ $ra = 94.3\%$



Table 2. (Continued)

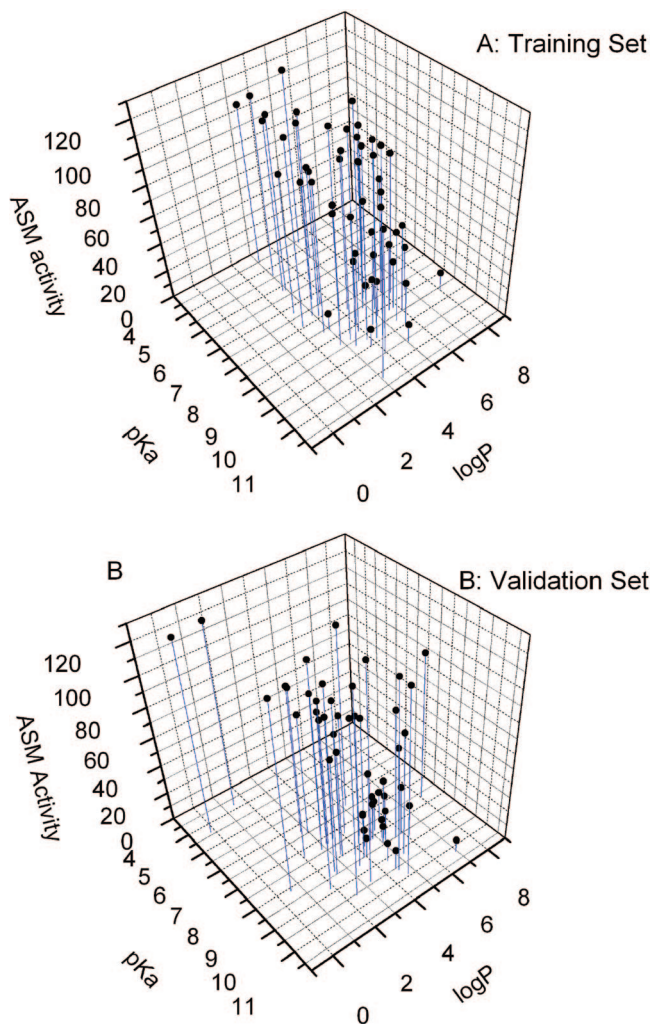
no	Structure	Generic name or substance code	no	Structure	Generic name or substance code
83		Procyclidine $pK_a = 10.49^a$ $\log P = 3.93^a$ $k = 4$ $ra = 85.4\%$	84		Promazine $pK_a = 9.34^{117}$ $\log P = 4.55^{59}$ $k = 2$ $ra = 33.6\%$
85		Protriptyline $pK_a = 10.61^a$ $\log P = 5.06^a$ $k = 1$ $ra = 12.7\%$	86		Ritanserin $pK_a = 8.20^{109}$ $\log P = 5.20^{109}$ $k = 13$ $ra = 108.3\%$
87		Sibutramin $pK_a = 9.69^a$ $\log P = 5.43^a$ $k = 2$ $ra = 63.2\%$	88		Tetracain $pK_a = 8.39^{61}$ $\log P = 3.73^{59}$ $k = 2$ $ra = 79.1\%$
89		Tofisopam $pK_a = 7.29^a$ $\log P = 2.40^a$ $k = 6$ $ra = 96.1\%$	90		Vinpocetine $pK_a = 7.80^a$ $\log P = 5.14^a$ $k = 6$ $ra = 109.9\%$

<sup>a</sup> Calculated value from the ACD/LogD Suite (program version 10.02, Toronto, Canada).<sup>75</sup> <sup>b</sup> Experimental data cited in the internal database of the ACD program. <sup>c</sup> In the case of two or more nitrogen atoms, the most basic nitrogen, as determined by the ACD/LogD Suite, is marked by an asterisk. The number of heavy atoms at the strongest basic nitrogen atom ( $k$ ) according to an algorithm is described in the Experimental Section.  $ra$ : residual ASM activity, compared to control conditions (=100%).

clomiphen 55, cloperastine 56, cyclobenzaprine 59, cyproheptadine 60, doxepin 63, drofenine 64, pimethixene 80, promazine 84, and protriptyline 85) reduced ASM activity in H4 cells to at least 50% (Figure 3A). Functional inhibition of ASM was found only for compounds with high  $pK_a$  ( $\geq 8.5$ ) and high  $\log P$  ( $\geq 3.0$ ) values. These physicochemical parameters appear to be a necessary precondition for functional inhibition of ASM. Since some compounds of the training set with high  $pK_a$  and high  $\log P$  values (alverine 40, antazoline 42, benfluorex 44, bromhexine 47, carbetapentane 51, cloricromen 57, cyclazocine 58, fluspirilene 68, mecamlamine 73, mibefradil 74, pimozone 81, pridinol 82, procyclidine 83, and sibutramin 87; Figure 3A) did not inhibit ASM activity, we conclude that  $pK_a \geq 8.5$  and  $\log P \geq 3.0$  are not sufficient preconditions for functional inhibition of ASM. We therefore tested steric hindrance of the cationic nitrogen atom as assessed by  $k$  as an additional predictor of functional inhibition of ASM. This third parameter significantly predicts whether or not a high  $pK_a$  and high  $\log P$  compound functionally inhibits ASM (ROC statistics: AUC = 0.806, SE = 0.082,  $P < 0.01$ ).

**Validation Set.** To verify the proposed influence of  $pK_a$ ,  $\log P$ , and  $k$  of a given substance on ASM activity, we tested a further 41 compounds which had not previously been tested for their ability to functionally inhibit ASM (compounds 91–131, Table 3) and 8 compounds from the literature set (amitriptyline

6, chlorpromazine 11, clomipramine 12, haloperidol 20, perhexiline 25, thioridazin 32, trihexyphenidyl 34, and trimipramine 35). The total validation set was comprised of 49 compounds with  $pK_a$  and  $\log P$  values  $\geq 4.79$  and  $\geq -0.19$ , respectively (Figure 3B). The experimental results obtained for the eight above-mentioned substances from the literature set, with the exception of trihexyphenidyl 34, were comparable to the previously published results. While trihexyphenidyl 34 was reported to functionally inhibit ASM,<sup>37</sup> we found no inhibition in our model system. This underlines the preliminary character of the results gathered from the literature set and the necessity to experimentally determine the inhibition of ASM under identical and defined conditions with training and validation sets. All compounds of the validation set that resulted in a more than 50% functional inhibition of ASM were found to have physicochemical characteristics predicted by the training set, namely, high  $pK_a$  and high  $\log P$  values. These compounds were chlorprothixene 94, fendiline 102, fluoxetine 104, maprotiline 109, norfluoxetine 113, nortriptyline 114, paroxetine 118, promethazine 120, sertraline 124, suloctidil 125, terfenadine 127, and trifluopromazine 129. Again, in agreement with the training set, these physicochemical parameters appear to be a necessary but not a sufficient precondition for functional inhibition of ASM since some of the compounds of the validation set with high  $pK_a$  ( $\geq 8.5$ ) and high  $\log P$  ( $\geq 3.0$ ) values (dicyclomine 98,



**Figure 3.** A tridimensional  $pK_a$ – $\log P$  property–activity diagram showing the distribution of the substances in the parameter space; (A) training set, (B) validation set. ASM activity indicates residual activity (%) compared to control conditions (=100%).

diphenhydramine **99**, diphenylpyraline **100**, donepezil **101**, lercanidipine **108**, mebeverine **110**, memantine **111**, oxymetazoline **116**, oxyphencyclimine **117**, pyrilamine **121**, triprolidine **130**, and xylometazoline **131**; Figure 3B) did not inhibit ASM activity. Thus, 18 of 31 high  $pK_a$  and high  $\log P$  compounds (58%) in the validation set are functional inhibitors of ASM. In agreement with the results obtained in the training set, steric hindrance of the cationic nitrogen as assessed by  $k$  significantly predicts whether or not a high  $pK_a$  and high  $\log P$  compound functionally inhibits ASM (ROC statistics: AUC = 0.726, SE = 0.098,  $P < 0.05$ ).

**The Significance of the SPAR Model.** We found high  $pK_a$  and high  $\log P$  values are necessary but not sufficient preconditions for functional ASM inhibition (Figures 2, 3A,B). The boundaries of the physicochemical parameters derived from the training set ( $pK_a \geq 8.5$  and  $\log P \geq 3.0$ ) make sense in the context of lysosomal accumulation and functional inhibition of ASM. Compounds with  $pK_a$  values above 8 cumulate to a maximal degree in lysosomes.<sup>6</sup> The location of all functional ASM inhibitors within a narrow area of the  $pK_a$ – $\log P$  parameter space verifies the physicochemical parameters selected and verifies lysosomal trapping as an important prerequisite resulting in functional inhibition of ASM.

Our results show that functional inhibition of ASM does not depend on a specific molecular drug class and is found in

tricyclic substances, monocyclic substances, and butyrophe-nones. Furthermore, functional ASM inhibition is not specific for a certain clinical action and is found, for instance, in antidepressant drugs, neuroleptic drugs, and drugs of abuse. However, this does not mean that functional inhibition of ASM is completely independent of certain molecular structures. In both the training and validation sets, the  $k$  values significantly predicted functional inhibition of ASM in compounds with high  $pK_a$  and high  $\log P$  values. From this, we conclude that, besides high  $pK_a$  and high  $\log P$  values, special structural preconditions are necessary for functional inhibition of ASM.

We then determined optimal cutoff values using all of the experimental data of the training set and validation set ( $n = 101$  compounds) and decision tree statistics. Using this approach, all three variables had a significant effect in predicting functional inhibition of ASM. The importance of the variables to predict functional inhibition of ASM decreases in the order  $pK_a > \log P > k$ . Optimal cutoff values for  $pK_a > 8.45$ ,  $\log P > 3.61$ , and  $k \leq 4$  were determined, which resulted in a prediction accuracy of 89% in our SPAR model. With this result, the structures of the prototypical functional ASM inhibitors, such as desipramine **17** ( $k = 1$ ) or amitriptyline **6** ( $k = 2$ ), appeared as if they had been designed to functionally inhibit ASM. While the lipophilic ring structure is embedded in the inner leaf of the lysosomal membrane, the cationic amino group is linked through an aliphatic chain like a fishing rod and is thus presented to the inner surface of the lysosome without steric hindrance.

The present approach to predict functional inhibition of ASM is based on clear physical–chemical principles. On the basis of the results presented here, new functional ASM inhibitor candidates might easily be identified. Each of the identified factors,  $pK_a$ ,  $\log P$ , and  $k$ , contributes significantly to predict functional inhibition of ASM. Although their combined use in the total experimental data set results in a prediction accuracy of 89%, the SPAR model does not allow a precise prediction at the level of an individual compound. Further studies are needed in order to more precisely describe the molecular characteristics explaining functional inhibition of ASM in high  $pK_a$  and high  $\log P$  compounds and in order to develop an improved quantitative structure–activity relationship.

#### Clinical Implications of the Findings Presented Here. (1)

Agents that reduce ASM and ceramide levels tend to attenuate receptor-mediated apoptosis, stress stimuli-induced apoptosis, and growth-factor-deprivation-mediated apoptosis and promote cell proliferation.<sup>10,23,40–43</sup> Therefore, all functional ASM inhibitors potentially have antiapoptotic and neuroprotective effects. The novel drugs tested here as functional ASM inhibitors may therefore be used in the treatment of disorders linked to apoptosis and enhanced activity of ASM, for example, neurodegeneration occurring in ischemia, stroke, Alzheimer's dementia, Parkinson's disease, Chorea Huntington, glaucoma or alcohol dependence, in radiation- and chemotherapy-induced apoptosis, in human immunodeficiency virus type-1-induced apoptosis, in the endotoxic shock syndrome, and in liver cell death and anemia occurring in Wilson disease.

(2) ASM inhibition suppresses lipopolysaccharide-mediated release of inflammatory cytokines from macrophages, indicating a possible preventive or therapeutic role for ASM inhibitors in inflammatory bowel disease.<sup>44</sup>

(3) ASM-dependent production of ceramide plays a key role in the generation of pulmonary edema in acute lung injury.<sup>45</sup> Functional inhibitors of ASM might thus be of therapeutic value in acute lung injury.

Table 3. Validation Set<sup>c</sup>

no	Structure	Generic name or substance code	no	Structure	Generic name or substance code
91		Amantadine $pK_a = 10.55^{73}$ $\log P = 2.44^{59}$ $k = 0$ $ra = 115.7\%$	92		Atropine $pK_a = 9.84^{64}$ $\log P = 1.83^{59}$ $k = 1$ $ra = 91.8\%$
93		Bromperidol $pK_a = 8.25^a$ $\log P = 3.19^a$ $k = 12$ $ra = 90.9\%$	94		Chlorprothixene $pK_a = 8.84^{61}$ $\log P = 5.18^{59}$ $k = 2$ $ra = 22.4\%$
95		Citalopram $pK_a = 9.50^{118}$ $\log P = 2.51^a$ $k = 2$ $ra = 79.9\%$	96		Clozapine $pK_a = 7.70^{67}$ $\log P = 3.42^{67}$ $k = 1$ $ra = 114.7\%$
97		Dextro-methorphan $pK_a = 8.30^{62}$ $\log P = 4.11^a$ $k = 1$ $ra = 82.7\%$	98		Dicyclomine $pK_a = 9.24^a$ $\log P = 6.05^a$ $k = 4$ $ra = 57.7\%$
99		Diphen-hydramine $pK_a = 9.02^{119}$ $\log P = 3.27^{59}$ $k = 2$ $ra = 73.4\%$	100		Diphenylpyraline $pK_a = 8.90^b$ $\log P = 4.54^a$ $k = 1$ $ra = 84.1\%$
101		Donepezil $pK_a = 9.08^{120}$ $\log P = 4.71^a$ $k = 7$ $ra = 118.8\%$	102		Fendiline $pK_a = 9.04^{121}$ $\log P = 4.89^{121}$ $k = 8$ $ra = 25.2\%$
103		Flavoxate $pK_a = 7.30^{122}$ $\log P = 5.18^a$ $k = 5$ $ra = 120.6\%$	104		Fluoxetine $pK_a = 9.50^{24}$ $\log P = 4.05^{123}$ $k = 1$ $ra = 13.0\%$

Table 3. (Continued)

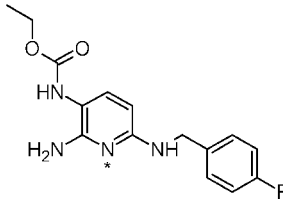
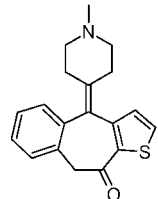
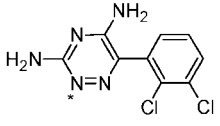
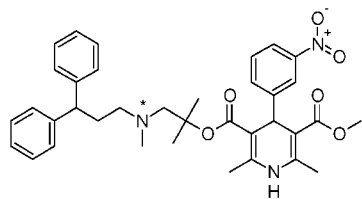
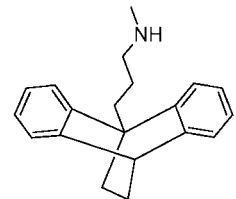
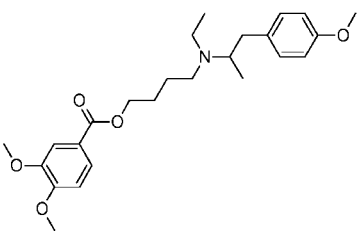

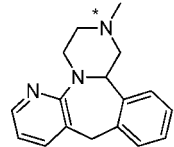
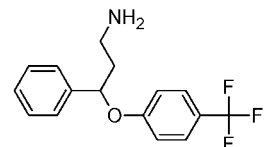
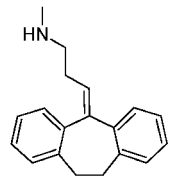
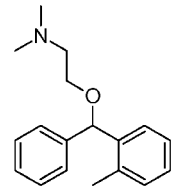
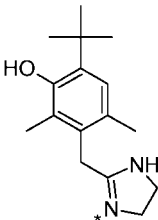
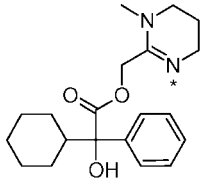
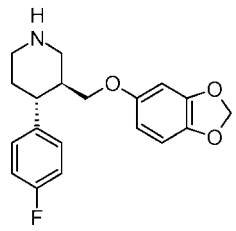
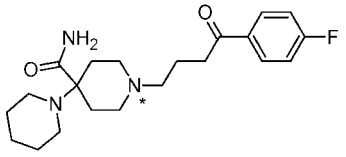
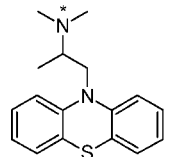
no	Structure	Generic name or substance code	no	Structure	Generic name or substance code
105		Flupirtine $pK_a = 4.79^a$ $\log P = 1.46^a$ $k = 6$ $ra = 124.1\%$	106		Ketotifen $pK_a = 8.24^{74}$ $\log P = 3.56^{74}$ $k = 1$ $ra = 105.1\%$
107		Lamotrigine $pK_a = 5.39^a$ $\log P = -0.19^a$ $k = 6$ $ra = 129.1\%$	108		Lercanidipine $pK_a = 8.66^a$ $\log P = 8.04^a$ $k = 16$ $ra = 99.1\%$
109		Maprotiline $pK_a = 10.50^{64}$ $\log P = 4.50^{67}$ $k = 1$ $ra = 13.5\%$	110		Mebeverine $pK_a = 9.51^a$ $\log P = 5.60^a$ $k = 13$ $ra = 88.0\%$
111		Memantine $pK_a = 10.42^{124}$ $\log P = 3.28^{59}$ $k = 0$ $ra = 75.6\%$	112		Mirtazapine $pK_a = 7.30^{64}$ $\log P = 2.75^a$ $k = 1$ $ra = 100.2\%$
113		Norfluoxetine $pK_a = 9.05^a$ $\log P = 4.36^a$ $k = 0$ $ra = 22.5\%$	114		Nortriptyline $pK_a = 10.10^{64}$ $\log P = 4.51^{125}$ $k = 1$ $ra = 13.3\%$
115		Orphenadrine $pK_a = 8.40^{62}$ $\log P = 3.77^{59}$ $k = 2$ $ra = 74.6\%$	116		Oxymetazoline $pK_a = 10.61^a$ $\log P = 4.52^a$ $k = 6$ $ra = 125.0\%$
117		Oxyphencyclimine $pK_a = 10.91^a$ $\log P = 4.69^a$ $k = 6$ $ra = 121.9\%$	118		Paroxetine $pK_a = 9.51^{64}$ $\log P = 3.89^a$ $k = 0$ $ra = 31.7\%$
119		Pipamperone $pK_a = 8.28^{113}$ $\log P = 2.02^{59}$ $k = 12$ $ra = 113.2\%$	120		Promethazine $pK_a = 9.10^{69}$ $\log P = 4.81^{59}$ $k = 2$ $ra = 32.2\%$

Table 3. (Continued)

no	Structure	Generic name or substance code	no	Structure	Generic name or substance code
121		Pyrilamine $pK_a = 8.92^{115}$ $\log P = 3.27^{59}$ $k = 2$ $ra = 103.7\%$	122		Reboxetine $pK_a = 8.37^a$ $\log P = 2.82^a$ $k = 0$ $ra = 105.3\%$
123		Selegeline $pK_a = 7.48^b$ $\log P = 2.95^a$ $k = 4$ $ra = 83.0\%$	124		Sertraline $pK_a = 9.16^{71}$ $\log P = 4.30^{71}$ $k = 1$ $ra = 12.3\%$
125		Suloctidil $pK_a = 9.69^a$ $\log P = 6.14^a$ $k = 8$ $ra = 21.9\%$	126		Sulpiride $pK_a = 9.12^{113}$ $\log P = 0.42^{65}$ $k = 2$ $ra = 99.2\%$
127		Terfenadine $pK_a = 8.60^{115}$ $\log P = 5.69^{115}$ $k = 15$ $ra = 21.8\%$	128		Tramadol $pK_a = 9.37^b$ $\log P = 2.51^{59}$ $k = 2$ $ra = 103.9\%$
129		Triflupromazine $pK_a = 9.20^{61}$ $\log P = 5.35^{59}$ $k = 2$ $ra = 29.5\%$	130		Triprolidine $pK_a = 9.69^{105}$ $\log P = 3.47^{74}$ $k = 4$ $ra = 117.9\%$
131		Xylometazoline $pK_a = 10.20^{126}$ $\log P = 5.26^a$ $k = 6$ $ra = 83.8\%$			

<sup>a</sup> Calculated value from the ACD/LogD Suite (program version 10.02, Toronto, Canada).<sup>75</sup> <sup>b</sup> Experimental data cited in the internal database of the ACD program. <sup>c</sup> In the case of two or more nitrogen atoms, the most basic nitrogen, as determined by the ACD/LogD Suite, is marked by an asterisk. The number of heavy atoms at the strongest basic nitrogen atom ( $k$ ) according to an algorithm is described in the Experimental Section.  $ra$ : residual ASM activity, compared to control conditions (=100%). Eight compounds from the literature set (amitriptyline **6**, chlorpromazine **11**, clomipramine **12**, haloperidol **20**, perhexiline **25**, thioridazin **32**, trihexyphenidyl **34**, trimipramine **35**) are also part of the validation set. Their experimental values are given in Table 1.

(4) In a pilot study, over-activity of ASM was found in patients suffering from major depression.<sup>19</sup> According to the “ceramide hypothesis for major depression”, over-activity of ASM leads to enhanced actions of ceramide in major depressive disorder. Functional ASM inhibitors might thereby contribute to antidepressant effects.

(5) The newly discovered functional ASM inhibitors were amlodipine **41**, astemizole **43**, benztropine **45**, bepridil **46**, camylofin **50**, chlorprothixene **94**, clomiphen **55**, cloperastine **56**, cyclobenzaprine **59**, cyproheptadine **60**, doxepine **63**,

drofenine **64**, fendiline **102**, fluoxetine **104**, maprotiline **109**, norfluoxetine **113**, nortriptyline **114**, paroxetine **118**, pimethixene **80**, promazine **84**, promethazine **120**, protriptyline **85**, sertraline **124**, suloctidil **125**, terfenadine **127**, and triflupromazine **129** (Figures 2, 3A,B). The U.S. FDA-approved drug list<sup>46</sup> indicates that many of these newly discovered functional ASM inhibitors are either in clinical use (**41**, **45**, **55**, **59**, **60**, **63**, **85**, **104**, **109**, **114**, **118**, **120**, and **124**) or are FDA-approved but no longer in active clinical use (**46**, **84**, and **94**). Astemizole **43**, camylofin **50**, cloperastine **56**, drofenine **64**, fendiline **102**,



the fluoxetine metabolite, norfluoxetine **113**, pimehixene **80**, sulotidil **125**, terfenadine **127**, and trifluopromazine **129** are substances not contained in the FDA-approved drug list. All of the newly defined functional ASM inhibitors, with the exception of drofenine **64** and norfluoxetine **113**, are included in the WHO drug list of approved and essential medicines.<sup>47</sup> The drugs tested here appear to offer major advantages as functional ASM inhibitors. Most of these substances are clinically available and are FDA-approved. These substances possess a low toxicity and a long-term clinical experience with their use is available. Some of these drugs have been in use for the last five decades. This suggests the potential for rapid advancement into preclinical and/or clinical trials. Most of these drugs appear capable of crossing the blood–brain barrier.

(6) The potential impact of confounding medication has to be considered in future clinical studies focusing on ASM activity. The results presented here may help to estimate the effect of a co-medication on ASM activity in such clinical trials.

**Limitations of the Findings Presented Here.** (1) Apart from substance-related variables ( $pK_a$  and  $\log P$ ), uptake into lysosomes depends on the extralysosomal concentration, which is closely associated with treatment-related variables (e.g., dosing of the compound) and organism-related variables (e.g., the pH difference between intra- and extralysosomal space, metabolism, protein binding, and transport processes). Whether or not a substance acts as an ASM inhibitor under therapeutic conditions in vivo depends on the interplay between these compounds and treatment- and organism-related variables. For example, a drug with physicochemical properties indicative of functional ASM inhibition may nevertheless be inactive under therapeutic conditions when the therapeutic extralysosomal concentration is extremely low. The SPAR model should therefore be interpreted in the context of therapeutic drug concentrations, which was not investigated here. The therapeutic concentrations of the drugs investigated here are usually in the low micromolar to submicromolar range. Mean fluoxetine **104** plasma concentrations, for example, are 80 ng/mL (0.26  $\mu$ M), with a dose of 20 mg/day, and 195 ng/mL (0.63  $\mu$ M), with a dose of 40 mg/day.<sup>48</sup> Future studies should clarify whether therapeutic drug concentrations result in a functional inhibition of ASM in vivo or not.

(2) The borders of the physicochemical and structural parameters ( $pK_a > 8.45$ ,  $\log P > 3.61$ ,  $k \leq 4$ ) are only valid with the special experimental conditions used here, namely, using 10  $\mu$ M concentrations of the compounds, 30 min incubation time, and cultured H4 cells as a model system. Using other concentrations of test substances, other incubation times, or other cell types might result in other borders of the physicochemical parameters.

(3) Besides the three identified molecular descriptors ( $pK_a$ ,  $\log P$ , and  $k$ ), other parameters might be associated with lysosomal accumulation and functional inhibition of ASM, namely, the largest conjugated fragment and conjugated bond number parameters,<sup>49</sup> the notational hydrogen-bonding capacity,<sup>50</sup> the number of alkyl substituents at a basic nitrogen atom,<sup>51</sup> the pH-dependent membrane permeability,<sup>52</sup> molar refractivity<sup>53</sup> or molecular weight, all of which were not considered here in order to keep the analysis simple and in order to concentrate on previously established parameters ( $pK_a$  and  $\log P$ ), with an obvious and strong influence on lysosomal drug concentration. Furthermore, the use of a higher number of independent factors in the present SPAR study is not meaningful, given the number of 52 different molecules with an experimentally determined effect on ASM activity within the training set. A higher number of substances with a known effect on ASM activity would be

necessary in order to clearly evaluate the independent effect of further molecular descriptors.

(4) The ACD program estimates  $pK_a$  values that correspond to dilute solutions of the bases at 25 °C. The true  $pK_a$  values occurring at 37 °C and at high ionic strength attained within lysosomes could be different.<sup>54</sup>

(5) For various reasons, the boundaries of the SPAR model must be taken as approximations. First, since a model, no matter how robust and statistically significant, is based on a limited training set, it is not expected to be applicable to every chemical. Second, the physicochemical constants used in the present investigation, where experimental values were not available, are calculated estimates with an associated error for those substances. In future studies, the currently provisional boundaries of the  $\log P$ ,  $pK_a$ , and  $k$  parameter space should be further investigated in order to define the boundaries more precisely by using a larger and structurally more heterogeneous set of compounds.

## Experimental Section

**Selection of Compound-Related Physicochemical Properties.** According to previously published results, functional ASM inhibition occurs if a weak basic drug reaches high lysosomal concentrations.<sup>21</sup> We therefore looked for compound-related physicochemical properties correlated to lysosomotropism. According to the pH partitioning theory,<sup>3,5,6</sup> the lysosomal concentration of a weak basic drug rises with higher  $pK_a$  values, up to  $pK_a$  values of approximately 8.5. The cumulation of weak basic drugs in lysosomes also depends on the lipophilicity of the compound.<sup>6,26,27,49,55–58</sup> With this hypothesis-driven approach, the following compound-related physicochemical parameters were selected as a basis for the SPAR model for functional inhibition of ASM: (1) the acid–base strength (negative logarithm of the equilibrium constant for the free base–protonated base reaction,  $pK_a$ ), and (2) the hydrophilicity–lipophilicity of a probe in the uncharged form (logarithm of the water–octanol partition coefficient,  $\log P$ ).

**Estimation of Compound-Related Physicochemical Properties.** Experimentally determined  $pK_a$  and  $\log P$  values were obtained from the classical  $\log P$  compilation by Hansch et al.,<sup>59</sup> from review articles,<sup>60–63</sup> from compilations devoted to the volume of distribution of licensed drugs,<sup>64–70</sup> from original research articles (for examples, see refs 71–74), and from the internal databases of the ACD/LogD Suite (program version 10.02, Toronto, Canada).<sup>75</sup> However, data were not available for all of the substances included in the literature and in the training and the validation sets. Consequently, experimental  $pK_a$  and  $\log P$  values were used wherever available and calculated for all other substances. Molecular structures were obtained from the PubChem-Project page<sup>76</sup> and analyzed by the ACD/LogD Suite. The “approximated apparent  $pK_a$  values” were used. The ACD/LogD Suite estimates  $pK_a$  values that correspond to dilute solutions of the bases at 25 °C. If tautomeric forms of a molecule were available, the structures were used in the form presented on the PubChem-Project page. In the case that there was more than one proton-accepting center in a single molecule, the one with the highest  $pK_a$  value (the most basic nitrogen atom) was used for SPAR model generation and statistical analysis. Structures without any proton-accepting site were excluded from further analysis.

The  $pK_a$  prediction algorithms of the ACD program are based on a fragmental method using generic substructures and Hammett-type equations to cover the most popular ionizable functional groups, using either a database or the estimation of electronic substituent constants. Steric effects are calculated by the modified branching equation. Furthermore, tautomeric equilibria, covalent hydration, and vinylology are taken into account where applicable.<sup>77</sup> Further details of the  $pK_a$  prediction algorithm are presented on the ACD webpage.<sup>75</sup> The  $\log P$  prediction algorithms of the ACD program are based on a fragmental method with correction factors.<sup>78</sup>

The congruence between experimental and calculated  $\log P$  values may be assessed using the Mannhold criteria,<sup>79</sup> which are defined as follows; absolute values of the individual differences between experimental and calculated  $\log P$  values  $<0.5$  are evaluated as acceptable, between 0.5 and 1 as disputable, and differences exceeding 1 as unacceptable.<sup>79</sup> While these criteria were used for the evaluation of  $\log P$  values, we used the same categorization of differences between experimental and calculated values for the evaluation of  $pK_a$  values. According to the Mannhold criteria, the congruence between  $pK_a$  and  $\log P$  values calculated by the ACD program and experimental values of the compounds within all three sets (literature set, the training set, and validation set; Tables 1–3) was good (absolute differences between calculated and experimental values were  $pK_a < 0.5$ , 54;  $pK_a = 0.5$ –1, 20;  $pK_a > 1$ , 4;  $\log P < 0.5$ , 43;  $\log P = 0.5$ –1, 13;  $\log P > 1$ , 11). Zero-intercept regressions between experimental and calculated values also indicated a good congruence ( $pK_a$ :  $n = 78$ , slope = 0.998,  $R^2 = 0.997$ ;  $\log P$ :  $n = 67$ , slope = 0.986,  $R^2 = 0.973$ ). The average absolute difference between experimental and calculated values was 0.39  $pK_a$  and 0.49  $\log P$  units, respectively.

We also used other methods to estimate  $\log P$  and  $pK_a$  values, namely,  $\log P$  and  $pK_a$  values provided by SPARC<sup>80–82</sup> and the Xlog  $P$  (version 2.0) values<sup>83</sup> provided at the PubChem-Project page. While the SPARC algorithm resulted in poorer predictions of  $pK_a$  and  $\log P$  values, the Xlog  $P$  (version 2.0) algorithm resulted in a comparable quality of prediction of  $\log P$  values (data not shown).

According to the literature, the prediction of  $pK_a$  values using the ACD program correlates well with experimentally determined values of antidepressant drugs.<sup>84</sup> Further comparisons between ACD-calculated and experimentally determined  $pK_a$  values are available on the ACD website.<sup>75</sup> The ability of the ACD program to accurately predict  $pK_a$  values was also confirmed by our comparison of experimental and ACD-calculated values within the literature, training, and validation sets of compounds. The  $\log P$  values calculated using the ACD/LogD Suite were close to experimental values within all three sets of compounds, consistent with the literature.<sup>78,85–87</sup> It therefore appeared appropriate to use ACD/LogD Suite-calculated  $pK_a$  and  $\log P$  values when experimental values were not available. The ambit of the ACD/LogD Suite covered all of the molecules investigated here, that is, small molecules with elements such as H, C, O, Cl, F, N, and Br.

**Algorithms for Estimation of Steric Hindrance at the Most Basic Nitrogen Atom ( $k$ ).** The algorithms were as follows: (1) Identify the most basic nitrogen atom, for example, by means of the ACD/LogD Suite. This nitrogen atom will be protonated first under acidic conditions. (2) The largest substituent at the most basic nitrogen atom as assessed by heavy atom count is not further looked at because this substituent is assumed to bind to and partition into the inner leaf of the lysosomal membrane. (3) The  $k$  is the heavy atom count at the remaining two substituents at the most basic nitrogen atom (examples:  $k = 1$  for desipramine **17**,  $k = 2$  for clomipramine **12**, and  $k = 11$  for benfluorex **44**). Heavy atoms means all atoms except hydrogen. (4) Several special situations occur if the most basic nitrogen atom is located in a ring system: (a) The nitrogen atom is a member of a single ring and does not carry a double bond. In this case, the bonds between the nitrogen atom and its neighbor atoms are cleaved, and the nitrogen atom is deleted. The number of heavy atoms of the smaller fragment, that is, the fragment having less heavy atoms, determines the  $k$  value (examples:  $k = 4$  for procyclidine **83** and  $k = 1$  for diphenylpyraline **100**). (b) The nitrogen atom is common of two annulated rings (examples: reserpine **29** and vinpocetine **90**). (c) The nitrogen atom is a part of three rings. This case does not occur in our study. (d) The nitrogen atom is part of a ring and carries a double bond (examples: harmine **69** and tofisopam **89**). We assigned a fixed value of 6 to the  $k$  value in the cases of (b)–(d) as a penalty for poor steric accessibility of the nitrogen atom [cases (b) + (c)] or for mesomeric delocalization of the positive charge of the protonated nitrogen atom [case (d)]. The range of  $k$  values was 0–18 in the

training set and 0–15 in the validation set. The  $k$  value of 3 occurred neither in the training set nor in the validations set.

**Set Selected from the Literature: Compounds with an Established Effect on ASM.** This set consists of compounds with proven and already published effects on ASM activity (Table 1, substances **1–38**, Figure 2). These substances were identified by means of a literature search using PubMed and subsequent screening of the reference lists of identified publications. If only a single concentration of a substance had been investigated in order to determine its effect as a functional ASM inhibitor, substances with a 50% or more reduction in ASM activity were valued as functional ASM inhibitors. Compounds with obvious pharmacodynamic effects on ASM different from those investigated here were omitted from the training set. For example, substances with oxidative properties, for example, daunorubicin,<sup>88</sup> were omitted because of their well-known direct activating effect on ASM<sup>89</sup> and ionophors<sup>90</sup> as they change the ionic composition and may therefore change ASM activity independent of lysosomotropism. Four substances which were negatively tested for functional inhibition of ASM activity, namely, 2-OH-, 7-OH-, 8-OH-chlorpromazine, and 2-OH-thiopropazine,<sup>34</sup> were not available on the PubChem site and were therefore excluded from the analysis. Furthermore, zwitterionic substances such as benzoylecgonine<sup>35</sup> were excluded since they do not enter the lysosome because they are charged at cytoplasmic pH. The set selected from the literature thus comprised 38 compounds (Table 1, Figure 2). Data for functional inhibition of ASM were taken from Albouz et al. (1981)<sup>17</sup> for imidodibenzyle **22**; from Albouz et al. (1986)<sup>34</sup> for 2-hydroxy-imipramine **1**, 10-hydroxy-imipramine **3**, amitriptyline **6**, and thiopropazine **31**; from Lejoyeux et al. (1991)<sup>37</sup> for alimemazine **4**, cyamemazine **15**, propericiacine **27**, and trihexyphenidyl **34**; from Nassogne et al. (2004)<sup>35</sup> for cocaine **13**; from Jaffré zou et al. (1995)<sup>38</sup> for amiodarone **5**, fantofarone (SR33557) **19**, perhexiline **25**, prochlorperazine **26**, quinacrine **28**, tamoxifene **30**, thioridazine **32**, and verapamil **36**; from Yoshida et al. (1985)<sup>18</sup> for AY9944 **7**, carbamazepine **9**, chloroquine **10**, chlorpromazine **11**, clomipramine **12**, desipramine **17**, dibucaine **18**, imipramine **23**, mianserine **24**, trifluoperazine **33**, trimipramine **35**, and W-5 **37**; from Sakuragawa et al. (1987)<sup>39</sup> for azacytidine **8**, colcemide **14**, cycloheximide **16**, and hydroxyurea **21**; from Spencer and Spence (1983)<sup>36</sup> for 6-hydroxy-dopamine **2**, haloperidole **20**, and reserpine **29**; and from Masson et al. (1992)<sup>91</sup> for W-7 **38**. Not all substances were independent of each other; 2-hydroxy-imipramine **1** and 10-hydroxy-imipramine **3** are metabolites of imipramine **23**. Three substances included in this set (AY9944 **7**, chloroquine **10**, and quinacrine **28**) possessed two nitrogen atoms with  $pK_a$  values above 6, that is, for these compounds, two nitrogen atoms will be protonated at an intralysosomal pH.

**Training Set.** Guided by the results obtained from the literature set, as shown in Figure 2, we selected a training set of 52 compounds with high  $\log P$  and high  $pK_a$  values, which had not been previously tested to functionally inhibit ASM activity (Table 2, compounds **39–90**, Figure 3A). The selection of compounds was governed by the inclusion of compounds from different structural classes and different clinical indications and compound availability.

**Validation Set.** According to the SPAR model based on the training set, we aimed to predict the compounds' abilities to functionally inhibit ASM activity. For this purpose, we selected a validation set of compounds, namely, 41 substances that have previously not been tested for their ability to functionally inhibit ASM activity (Table 3, substances **91–131**, Figure 3B). The selection of compounds was governed by the inclusion of compounds from different structural classes and different clinical indications and compound availability and on the basis of our previous experiences with some of these compounds.<sup>92–96</sup> Furthermore, we also experimentally determined the extent of functional inhibition of ASM in eight substances contained in the literature set (amitriptyline **6**, chlorpromazine **11**, clomipramine **12**, desipramine **17**, haloperidol **20**, perhexiline **25**, thioridazine **32**, trihexyphenidyl **34**, and trimipramine **35**). Not all substances are independent of each other; memantine **111** is the dimethyl derivative



of amantadine **91**, norfluoxetine **113** is the desmethyl derivative of fluoxetine **104**, oxymetazoline **116** is the hydroxy derivative of xylometazoline **131**, and nortriptyline **114** is the desmethyl derivative of amitriptyline **6**.

**Chemicals.** All substances were obtained from Sigma-Aldrich (Munich, Germany), except for benztropine (**45**), dextromethorphan (**97**), and donepezil (**101**), which were purchased from VWR International (Ismaning, Germany), and sertraline (**124**) and sibutramine (**87**), which were purchased from Biotrend Chemikalien (Köln, Germany). All compounds were purchased in the highest purity available.

**Cell Culture.** Human brain neuroglioma H4 cells were purchased from Promochem (Wesel, Germany), and rat neuroendocrine pheochromocytoma PC12 cells were from ECACC (Porton Down, U.K.). The H4 cells were cultivated in DMEM medium (Biochrom) supplemented with 10% (v/v) FBS, 1% (v/v) penicillin/streptomycin antibiotics (Biochrom), and 4 mM glutamine (Biochrom). The PC12 cells were cultivated in RPMI medium (Biochrom, Berlin, Germany) supplemented with 10% (v/v) fetal bovine serum (FBS), 1% (v/v) penicillin/streptomycin antibiotics (Biochrom), and 2 mM glutamine (Biochrom). To facilitate adherent growth of PC12 cells, culture flasks were coated with 8  $\mu\text{g}/\text{cm}^2$  collagen IV (Roche, Mannheim, Germany) in PBS (Biochrom) for at least 4 h prior to seeding of the cells. Both cell lines were kept at 37 °C in a humidified atmosphere at 5%  $\text{CO}_2$  and were routinely split at a ratio of 1:6 and 1:4 for H4 and PC12 cells, respectively.

**Experimental Determination of ASM Activity.** The activity of ASM was determined in whole-cell lysates, as previously described.<sup>97</sup> Briefly, H4 and PC12 cells were seeded in 6 well dishes and grown to a confluence of 80–90%. After the substances were added to the respective growth medium at a final concentration of 10  $\mu\text{M}$ , cells were kept at 37 °C in humidified atmosphere at 5%  $\text{CO}_2$  for a further 30 min (DMEM pH 7.6; RPMI pH 7.5). Cells were washed with PBS (Biochrom) and lysed in 100  $\mu\text{L}$  of lysis buffer [250 mM sodium acetate, pH 5.0 (Merck, Darmstadt, Germany), 0.1% NP-40 (Sigma-Aldrich), 1.3 mM EDTA (Sigma-Aldrich), 1 tablet of complete mini protease inhibitor mix/10 mL (Roche)] for 20 min at 4 °C. Cell debris was removed by centrifugation at 10000g for 15 min at 4 °C. Quantitative analysis of ASM activity was performed on 10–50  $\mu\text{g}$  of total cellular protein extract and diluted in 250  $\mu\text{L}$  of lysis buffer; 440 pmol [choline methyl-<sup>14</sup>C]sphingomyelin (Perkin-Elmer, MA) was suspended in 30  $\mu\text{L}$  of enzyme buffer [250 mM sodium acetate pH 5.0 (Merck), 0.1% NP-40 (Sigma-Aldrich), 1.3 mM EDTA (Sigma-Aldrich)] and added to the protein extract. The enzymatic reaction was incubated at 37 °C for 20 min. The reaction was stopped by addition of 800  $\mu\text{L}$  of chloroform/methanol (2:1), and phases were separated by centrifugation. Radioactivity of the aqueous phase was quantified by liquid scintillation counting and enabled quantification of ASM activity. Results are given as ASM activity, based on the respective control reactions. The results refer to the mean values resulting from three independent experiments, each with a coefficient of variation of approximately 17%. All experiments were analyzed by a technician who was unaware of the expected results. A more than 50% inhibition of ASM activity in H4 cells was rated as positive. All compounds of the training and validations sets, as well as eight substances from the literature set, were tested in H4 cells. A subgroup of the validation set was, in addition, tested in PC12 cells (**91–97**, **99**, **104**, **105**, **107**, **109**, **111–115**, **118–124**, **126**, **128**, and **129**). The correlation between residual ASM activity for the 27 compounds measured in both H4 and PC12 cells was 0.72,  $P < 0.001$  (data not shown).

**Statistical Analysis.** Zero-intercept regressions, Spearman correlation coefficients, as well as exploratory statistics were computed for calculated and experimental log  $P$  and  $\text{pK}_a$  values. Nonparametric receiver operating characteristic (ROC) curves and the area under the curve (AUC) were used to measure the effectiveness of  $k$  in predicting functional inhibition of ASM in high  $\text{pK}_a$  and high log  $P$  compounds. A classification tree statistic (CART algorithm, maximum of 3 steps, equal a priori probability in all categories) was used to generate cutoff values using the total experimental data

set of both the training set and the validation set ( $n = 101$ ). A  $P$  value of less than 0.05 (two-tailed) was considered to indicate statistical significance. All statistical calculations were performed using SPSS (version 15, Chicago, IL),

**Acknowledgment.** We are indebted to anonymous referees, who gave valuable advice. We thank Andrea Leicht for excellent technical assistance, Torsten Kuwert (Department for Nuclear Medicine, University Hospital Erlangen) for support with the use of the radionucleotide facility, and Elisabeth Naschberger (Division of Molecular and Experimental Surgery, University Hospital Erlangen) for support with quantifying radioactivity. Our thanks to Heidi Joao for her support in proofreading the manuscript. The work was supported by grants from DFG (GU 335/10-3).

## References

- (1) Kaufmann, A. M.; Krise, J. P. Lysosomal sequestration of amine-containing drugs: Analysis and therapeutic implications. *J. Pharm. Sci.* **2007**, *96*, 729–746.
- (2) Mellman, I.; Fuchs, R.; Helenius, A. Acidification of the endocytic and exocytic pathways. *Annu. Rev. Biochem.* **1986**, *55*, 663–700.
- (3) de Duve, C.; de Barse, T.; Poole, B.; Trouet, A.; Tulkens, P.; van Hoof, F. Lysosomotropic agents. *Biochem. Pharmacol.* **1974**, *23*, 2495–2531.
- (4) Koenig, H. Lysosomes. In *Handbook of Neurochemistry*, 7th ed.; Lajtha, A., Ed.; Plenum Press: New York, 1984; pp 177–204.
- (5) MacIntyre, A.; Cutler, D. J. The potential role of lysosomes in tissue distribution of weak bases. *Biopharm. Drug Dispos.* **1988**, *9*, 513–526.
- (6) Trapp, S.; Rosania, G. R.; Horobin, R. W.; Kornhuber, J. Quantitative modeling of selective lysosomal targeting by passive diffusion of xenobiotic compounds—model development and simulations for single cells. **2007**, submitted.
- (7) Kornhuber, J.; Schultz, A.; Wiltfang, J.; Meineke, I.; Gleiter, C. H.; Zöchling, R.; Boissl, K.-W.; Leblhuber, F.; Riederer, P. Persistence of haloperidol in human brain tissue. *Am. J. Psychiatry* **1999**, *156*, 885–890.
- (8) Kornhuber, J.; Quack, G.; Danysz, W.; Jellinger, K.; Danielczyk, W.; Gsell, W.; Riederer, P. Therapeutic brain concentration of the NMDA receptor antagonist amantadine. *Neuropharmacology* **1995**, *34*, 713–721.
- (9) Kornhuber, J.; Weigmann, H.; Rörich, J.; Wiltfang, J.; Bleich, S.; Meineke, I.; Zöchling, R.; Aly, M.; Riederer, P.; Hiemke, C. Region specific distribution of levomepromazine in the human brain. *J. Neural Transm.* **2006**, *113*, 387–397.
- (10) Gulbins, E.; Li, P. L. Physiological and pathophysiological aspects of ceramide. *Am. J. Physiol.: Regul. Integr. Comp. Physiol.* **2006**, *290*, R11–R26.
- (11) Gulbins, E. Regulation of death receptor signaling and apoptosis by ceramide. *Pharmacol. Res.* **2003**, *47*, 393–399.
- (12) Schwarz, A.; Futerman, A. H. Distinct roles for ceramide and glucosylceramide at different stages of neuronal growth. *J. Neurosci.* **1997**, *17*, 2929–2938.
- (13) Futerman, A. H.; Hannun, Y. A. The complex life of simple sphingolipids. *EMBO Rep.* **2004**, *5*, 777–782.
- (14) Hobson, J. P.; Rosenfeldt, H. M.; Barak, L. S.; Olivera, A.; Poulton, S.; Caron, M. G.; Milstien, S.; Spiegel, S. Role of the sphingosine-1-phosphate receptor EDG-1 in PDGF-induced cell motility. *Science* **2001**, *291*, 1800–1803.
- (15) Spiegel, S.; Milstien, S. Sphingosine 1-phosphate, a key cell signaling molecule. *J. Biol. Chem.* **2002**, *277*, 25851–25854.
- (16) Toman, R. E.; Payne, S. G.; Watterson, K. R.; Maceyka, M.; Lee, N. H.; Milstien, S.; Bigbee, J. W.; Spiegel, S. Differential transactivation of sphingosine-1-phosphate receptors modulates NGF-induced neurite extension. *J. Cell Biol.* **2004**, *166*, 381–392.
- (17) Albouze, S.; Hauw, J. J.; Berwald-Netter, Y.; Boutry, J. M.; Bourdon, R.; Baumann, N. Tricyclic antidepressants induce sphingomyelinase deficiency in fibroblast and neuroblastoma cell cultures. *Biomedicine* **1981**, *35*, 218–220.
- (18) Yoshida, Y.; Arimoto, K.; Sato, M.; Sakuragawa, N.; Arima, M.; Satoyoshi, E. Reduction of acid sphingomyelinase activity in human fibroblasts induced by AY-9944 and other cationic amphiphilic drugs. *J. Biochem. (Tokyo)* **1985**, *98*, 1669–1679.
- (19) Kornhuber, J.; Medlin, A.; Bleich, S.; Jendrossek, V.; Henkel, A. W.; Wiltfang, J.; Gulbins, E. High activity of acid sphingomyelinase in major depression. *J. Neural Transm.* **2005**, *112*, 1583–1590.
- (20) Sakuragawa, N.; Sakuragawa, M.; Kuwabara, T.; Pentchev, P. G.; Barranger, J. A.; Brady, R. O. Niemann–Pick disease experimental

- model: sphingomyelinase reduction induced by AY-9944. *Science* **1977**, 196, 317–319.
- (21) Kölzer, M.; Werth, N.; Sandhoff, K. Interactions of acid sphingomyelinase and lipid bilayers in the presence of the tricyclic antidepressant desipramine. *FEBS Lett.* **2004**, 559, 96–98.
  - (22) Hurwitz, R.; Ferlinz, K.; Sandhoff, K. The tricyclic antidepressants desipramine causes proteolytic degradation of lysosomal sphingomyelinase in human fibroblasts. *Biol. Chem. Hoppe-Seyler* **1994**, 375, 447–450.
  - (23) Kolesnick, R. The therapeutic potential of modulating the ceramide/sphingomyelin pathway. *J. Clin. Invest.* **2002**, 110, 3–8.
  - (24) Kornhuber, J.; Retz, W.; Riederer, P. Slow accumulation of psychotropic substances in the human brain. Relationship to therapeutic latency of neuroleptic and antidepressant drugs. *J. Neural Transm. Suppl.* **1995**, 46, 311–319.
  - (25) Duvvuri, M.; Konkari, S.; Funk, R. S.; Krise, J. M.; Krise, J. P. A chemical strategy to manipulate the intracellular localization of drugs in resistant cancer cells. *Biochemistry* **2005**, 44, 15743–15749.
  - (26) Ishizaki, J.; Yokogawa, K.; Ichimura, F.; Ohkuma, S. Uptake of imipramine in rat liver lysosomes in vitro and its inhibition by basic drugs. *J. Pharmacol. Exp. Ther.* **2000**, 294, 1088–1098.
  - (27) Lemieux, B.; Percival, M. D.; Falgouty, J. P. Quantitation of the lysosomotropic character of cationic amphiphilic drugs using the fluorescent basic amine Red DND-99. *Anal. Biochem.* **2004**, 327, 247–251.
  - (28) Kolter, T.; Sandhoff, K. Principles of lysosomal membrane digestion: Stimulation of sphingolipid degradation by sphingolipid activator proteins and anionic lysosomal lipids. *Annu. Rev. Cell Dev. Biol.* **2005**, 21, 81–103.
  - (29) Möbius, W.; van, D. E.; Ohno-Iwashita, Y.; Shimada, Y.; Heijnen, H. F.; Slot, J. W.; Geuze, H. J. Recycling compartments and the internal vesicles of multivesicular bodies harbor most of the cholesterol found in the endocytic pathway. *Traffic* **2003**, 4, 222–231.
  - (30) Wilkening, G.; Linke, T.; Uhlhorn-Dierks, G.; Sandhoff, K. Degradation of membrane-bound ganglioside GM1. Stimulation by bis-(monoacylglycerol)phosphate and the activator proteins SAP-B and GM2-AP. *J. Biol. Chem.* **2000**, 275, 35814–35819.
  - (31) Linke, T.; Wilkening, G.; Lansmann, S.; Moczall, H.; Bartelsen, O.; Weisgerber, J.; Sandhoff, K. Stimulation of acid sphingomyelinase activity by lysosomal lipids and sphingolipid activator proteins. *Biol. Chem.* **2001**, 382, 283–290.
  - (32) Albouze, S.; Boutry, J. M.; Dubois, G.; Bourdon, R.; Hauw, J. J.; Baumann, N. Lipid and lysosomal enzymes in human fibroblasts cultured with perhexiline maleate. *Naunyn-Schmiedeberg's Arch. Pharmacol.* **1981**, 317, 173–177.
  - (33) Albouze, S.; Vanier, M. T.; Hauw, J. J.; Le, Saux, F.; Boutry, J. M.; Baumann, N. Effect of tricyclic antidepressants on sphingomyelinase and other sphingolipid hydrolases in C6 cultured glioma cells. *Neurosci. Lett.* **1983**, 36, 311–315.
  - (34) Albouze, S.; Le Saux, F.; Wenger, D.; Hauw, J. J.; Baumann, N. Modifications of sphingomyelin and phosphatidylcholine metabolism by tricyclic antidepressants and phenothiazines. *Life Sci.* **1986**, 38, 357–363.
  - (35) Nassogne, M. C.; Lizarraga, C.; N'Kuli, F.; Van Bambeke, F.; Van Binst, R.; Wallemacq, P.; Tulken, P. M.; Mingeot-Leclercq, M. P.; Levade, T.; Courtoy, P. J. Cocaine induces a mixed lysosomal lipidosis in cultured fibroblasts, by inactivation of acid sphingomyelinase and inhibition of phospholipase A1. *Toxicol. Appl. Pharmacol.* **2004**, 194, 101–110.
  - (36) Sperker, E. R.; Spence, M. W. Neutral and acid sphingomyelinases of rat brain: Somatotopographical distribution and activity following experimental manipulation of the dopaminergic system in vivo. *J. Neurochem.* **1983**, 40, 1182–1184.
  - (37) Lejoyeux, M.; Mazière, J. C.; Mora, L.; Auclair, M.; Mazière, C. Sphingomyelinase fibroblast activity and psychoactive drugs. *Biol. Psychiatry* **1991**, 30, 841–843.
  - (38) Jaffrézou, J. P.; Chen, G.; Durán, G. E.; Muller, C.; Bordier, C.; Laurent, G.; Sikic, B. I.; Levade, T. Inhibition of lysosomal acid sphingomyelinase by agents which reverse multidrug resistance. *Biochim. Biophys. Acta* **1995**, 1266, 1–8.
  - (39) Sakuragawa, N.; Sato, M.; Kamo, I.; Arima, M. Therapeutic effects of dipolar aprotic substances on Niemann–Pick cells. *Acta Paediatr. Jpn.* **1987**, 29, 433–440.
  - (40) Thevissen, K.; Francois, I. E.; Winderickx, J.; Pannecouque, C.; Cammue, B. P. Ceramide involvement in apoptosis and apoptotic diseases. *Mini. Rev. Med. Chem.* **2006**, 6, 699–709.
  - (41) Deigner, H. P.; Haberkorn, U.; Kinscherf, R. Apoptosis modulators in the therapy of neurodegenerative diseases. *Expert Opin. Invest. Drugs* **2000**, 9, 747–764.
  - (42) Pandey, S.; Murphy, R. F.; Agrawal, D. K. Recent advances in the immunobiology of ceramide. *Exp. Mol. Pathol.* **2006**.
  - (43) Raff, M. C.; Barres, B. A.; Burne, J. F.; Coles, H. S.; Ishizaki, Y.; Jacobson, M. D. Programmed cell death and the control of cell survival: Lessons from the nervous system. *Science* **1993**, 262, 659–700.
  - (44) Sakata, A.; Ochiai, T.; Shimeno, H.; Hikishima, S.; Yokomatsu, T.; Shibuya, S.; Toda, A.; Eyanagi, R.; Soeda, S. Acid sphingomyelinase inhibition suppresses lipopolysaccharide-mediated release of inflammatory cytokines from macrophages and protects against disease pathology in dextran sulphate sodium-induced colitis in mice. *Immunology* **2007**, 122, 54–64.
  - (45) Göggel, R.; Winoto-Morbach, S.; Vielhaber, G.; Imai, Y.; Lindner, K.; Brade, L.; Brade, H.; Ehlers, S.; Slutsky, A. S.; Schütze, S.; Gulbins, E.; Uhlig, S. PAF-mediated pulmonary edema: A new role for acid sphingomyelinase and ceramide. *Nat. Med.* **2004**, 10, 155–160.
  - (46) *Approved Drug Products with Therapeutic Equivalence Evaluations*; U.S. Department of Health and Human Services. Food and Drug Administration. Center for Drug Evaluation and Research. Office of Pharmaceutical Science. Office of Generic Drugs. 2007.
  - (47) The ATC/DDD System, The WHO Collaborating Centre for Drug Statistics Methodology. <http://www.whocc.no/atcddd/> (2007) Norwegian Institute of Public Health.
  - (48) Baumann, P.; Hiemke, C.; Ulrich, S.; Eckermann, G.; Gaertner, I.; Gerlach, M.; Kuss, H. J.; Laux, G.; Müller-Oerlinghausen, B.; Rao, M. L.; Riederer, P.; Zernig, G. The AGNP-TDM expert group consensus guidelines: Therapeutic drug monitoring in psychiatry. *Pharmacopsychiatry* **2004**, 37, 243–265.
  - (49) Horobin, R. W.; Stockert, J. C.; Rashid-Doubell, F. Fluorescent cationic probes for nuclei of living cells: Why are they selective? A quantitative structure–activity relations analysis. *Histochem. Cell Biol.* **2006**, 126, 165–175.
  - (50) Lloyd, J. B. Lysosome membrane permeability: Implications for drug delivery. *Adv. Drug Delivery Rev.* **2000**, 41, 189–200.
  - (51) Dubowchik, G. M.; Padilla, L.; Edinger, K.; Firestone, R. A. Amines that transport protons across bilayer membranes: Synthesis, lysosomal neutralization, and two-phase  $pK_a$  values by NMR. *J. Org. Chem.* **1996**, 61, 4676–4684.
  - (52) Duvvuri, M.; Gong, Y.; Chatterji, D.; Krise, J. P. Weak base permeability characteristics influence the intracellular sequestration site in the multidrug-resistant human leukemic cell line HL-60. *J. Biol. Chem.* **2004**, 279, 32367–32372.
  - (53) Zamora, J. M.; Pearce, H. L.; Beck, W. T. Physical–chemical properties shared by compounds that modulate multidrug resistance in human leukemic cells. *Mol. Pharmacol.* **1988**, 33, 454–462.
  - (54) Cookson, R. F. The determination of acidity constants. *Chem. Rev.* **1974**, 74, 5–28.
  - (55) Duvvuri, M.; Krise, J. P. A novel assay reveals that weakly basic model compounds concentrate in lysosomes to an extent greater than pH-partitioning theory would predict. *Mol. Pharm.* **2005**, 2, 440–448.
  - (56) Yokogawa, K.; Ishizaki, J.; Ohkuma, S.; Miyamoto, K. Influence of lipophilicity and lysosomal accumulation on tissue distribution kinetics of basic drugs: A physiologically based pharmacokinetic model. *Methods Find. Exp. Clin. Pharmacol.* **2002**, 24, 81–93.
  - (57) Ishizaki, J.; Yokogawa, K.; Nakashima, E.; Ohkuma, S.; Ichimura, F. Uptake of basic drugs into rat lung granule fraction in vitro. *Biol. Pharm. Bull.* **1998**, 21, 858–861.
  - (58) Rashid, F.; Horobin, R. W.; Williams, M. A. Predicting the behaviour and selectivity of fluorescent probes for lysosomes and related structures by means of structure–activity models. *Histochem. J.* **1991**, 23, 450–459.
  - (59) Hansch, C.; Leo, A.; Hoekman, D. *Exploring QSAR: Fundamentals and applications in chemistry and biology*; American Chemical Society: Washington, DC, 1995.
  - (60) Raymond, G. G.; Born, J. L. An updated  $pK_a$  listing of medicinal compounds. *Drug Intell. Clin. Pharm.* **1986**, 20, 683–686.
  - (61) Herzfelt, C. D. Dissoziationskonstanten von Arzneistoffen—Eine Übersichtstabelle. *Pharm. Ztg.* **1980**, 125, 608–614.
  - (62) Newton, D. W.; Kluza, R. B.  $pK_a$  values of medicinal compounds in pharmacy practice. *Drug Intell. Clin. Pharm.* **1978**, 12, 546–554.
  - (63) Albert, A.; Serjeant, E. P. *The Determination of Ionization Constants—A Laboratory Manual*; Chapman and Hall Ltd.: London, 1984; pp 2–218.
  - (64) Lombardo, F.; Obach, R. S.; Shalaeva, M. Y.; Gao, F. Prediction of human volume of distribution values for neutral and basic drugs. 2. Extended data set and leave-class-out statistics. *J. Med. Chem.* **2004**, 47, 1242–1250.
  - (65) Poulin, P.; Theil, F. P. Prediction of pharmacokinetics prior to in vivo studies. 1. Mechanism-based prediction of volume of distribution. *J. Pharm. Sci.* **2002**, 91, 129–156.
  - (66) De Buck, S. S.; Sinha, V. K.; Fenu, L. A.; Gilissen, R. A.; Mackie, C. E.; Nijssen, M. J. The prediction of drug metabolism, tissue



- distribution, and bioavailability of 50 structurally diverse compounds in rat using mechanism-based absorption, distribution, and metabolism prediction tools. *Drug Metab. Dispos.* **2007**, *35*, 649–659.
- (67) Rodgers, T.; Rowland, M. Mechanistic approaches to volume of distribution predictions: Understanding the processes. *Pharm. Res.* **2007**, *24*, 918–933.
- (68) Yokogawa, K.; Nakashima, E.; Ishizaki, J.; Maeda, H.; Nagano, T.; Ichimura, F. Relationships in the structure-tissue distribution of basic drugs in the rabbit. *Pharm. Res.* **1990**, *7*, 691–696.
- (69) Ishizaki, J.; Yokogawa, K.; Nakashima, E.; Ichimura, F. Prediction of changes in the clinical pharmacokinetics of basic drugs on the basis of octanol–water partition coefficients. *J. Pharm. Pharmacol.* **1997**, *49*, 762–767.
- (70) Rodgers, T.; Rowland, M. Physiologically based pharmacokinetic modelling 2: Predicting the tissue distribution of acids, very weak bases, neutrals and zwitterions. *J. Pharm. Sci.* **2006**, *95*, 1238–1257.
- (71) Deák, K.; Takás-Novák, K.; Tihanyi, K.; Noszá, B. Physico-chemical profiling of antidepressive sertraline: Solubility, ionisation, lipophilicity. *Med. Chem.* **2006**, *2*, 385–389.
- (72) Hansch, C.; Björkroth, J. P.; Leo, A. Hydrophobicity and central nervous system agents: On the principle of minimal hydrophobicity in drug design. *J. Pharm. Sci.* **1987**, *76*, 663–687.
- (73) Gelb, R. I.; Laufer, D. A. Acidic dissociation of amantadine hydrochloride. *J. Chem. Eng. Data* **1983**, *28*, 335–337.
- (74) Quinones-Torrel, C.; Sagrado, S.; Villanueva-Camanas, R. M.; Medina-Hernandez, M. J. Retention pharmacokinetic and pharmacodynamic parameter relationships of antihistamine drugs using biopartitioning micellar chromatography. *J. Chromatogr. B* **2001**, *761*, 13–26.
- (75) ACD/LogD Suite. <http://www.whocc.no/atcddd/> (2007) Advanced Chemistry Development Inc.
- (76) PubChem-Project. <http://pubchem.ncbi.nlm.nih.gov> (2007) National Center for Biotechnology Information, U.S.A.
- (77) Japertas, P.; Didziapetris, R.; Petrauskas, A. Fragmental methods in the analysis of biological activities of diverse compound sets. *Mini. Rev. Med. Chem.* **2003**, *3*, 797–808.
- (78) Petrauskas, A. A.; Kolovanov, E. A. ACD/Log P method description. *Perspect. Drug Discovery Des.* **2000**, *19*, 99–116.
- (79) Mannhold, R.; Dross, K. Calculation procedures for molecular lipophilicity: A comparative study. *Quant. Struct.-Act. Relat.* **1996**, *15*, 403–409.
- (80) SPARC Performs Automated Reasoning in Chemistry, version 3.1. <http://ibmlc2.chem.uga.edu/sparc/> (2007) University of Georgia: Athens, GA.
- (81) Hilal, S. H.; Karickhoff, S. W.; Carreira, L. A. A rigorous test for SPARC's chemical reactivity models: Estimation of more than 4300 ionization  $pK_a$ s. *Quant. Struct.-Act. Relat.* **1995**, *14*, 348–355.
- (82) Hilal, S. H.; Karickhoff, S. W.; Carreira, L. A. Prediction of the solubility, activity coefficient, and liquid/liquid partition coefficient of organic compounds. *QSAR Comb. Sci.* **2004**, *23*, 709–720.
- (83) Wang, R.; Gao, Y.; Lai, L. Calculating partition coefficient by atom-additive method. *Perspect. Drug Discovery Des.* **2000**, *19*, 47–66.
- (84) Ruiz, R.; Ràfols, C.; Rosés, M.; Bosch, E. A potentially simpler approach to measure aqueous  $pK_a$  of insoluble basic drugs containing amino groups. *J. Pharm. Sci.* **2003**, *92*, 1473–1481.
- (85) Mannhold, R.; van de Waterbeemd, H. Substructure and whole molecule approaches for calculating log P. *J. Comput. Aided Mol. Des.* **2001**, *15*, 337–354.
- (86) Mannhold, R. The impact of lipophilicity in drug research: A case report on beta-blockers. *Mini. Rev. Med. Chem.* **2005**, *5*, 197–205.
- (87) Buchwald, P.; Bodor, N. Octanol–water partition: Searching for predictive models. *Curr. Med. Chem.* **1998**, *5*, 353–380.
- (88) Jaffrézou, J. P.; Levade, T.; Bettaieb, A.; Andrieu, N.; Bezombes, C.; Maestre, N.; Vermeersch, S.; Rousse, A.; Laurent, G. Daunorubicin-induced apoptosis: Triggering of ceramide generation through sphingomyelin hydrolysis. *EMBO J.* **1996**, *15*, 2417–2424.
- (89) Qiu, H.; Edmunds, T.; Baker-Malcolm, J.; Karey, K. P.; Estes, S.; Schwarz, C.; Hughes, H.; Van Patten, S. M. Activation of human acid sphingomyelinase through modification or deletion of C-terminal cysteine. *J. Biol. Chem.* **2003**, *278*, 32744–32752.
- (90) Sakuragawa, N.; Mito, T.; Kawada, A. Niemann–Pick disease: Coupling and uncoupling of inhibited sphingomyelinase activity and exogenous cholesterol esterification in fibroblasts by ionophore treatment. *Biochim. Biophys. Acta* **1994**, *1213*, 193–198.
- (91) Masson, M.; Spezzatti, B.; Chapman, J.; Battisti, C.; Baumann, N. Calmodulin antagonists chlorpromazine and W-7 inhibit exogenous cholesterol esterification and sphingomyelinase activity in human skin fibroblast cultures. Similarities between drug-induced and Niemann–Pick type C lipidoses. *J. Neurosci. Res.* **1992**, *31*, 84–88.
- (92) Kornhuber, J.; Parsons, C. G.; Hartmann, S.; Retz, W.; Kamolz, S.; Thome, J.; Riederer, P. Orphenadrine is an uncompetitive N-methyl-D-aspartate (NMDA) receptor antagonist: Binding and patch clamp studies. *J. Neural Transm.: Gen. Sect.* **1995**, *102*, 237–246.
- (93) Kornhuber, J.; Herr, B.; Thome, J.; Riederer, P. The antiparkinsonian drug bupropion binds to NMDA and sigma receptors in postmortem human brain tissue. *J. Neural Transm. Suppl.* **1995**, *46*, 131–137.
- (94) Kornhuber, J.; Bleich, S.; Wiltfang, J.; Maler, M.; Parsons, C. G. Flupirtine shows functional NMDA receptor antagonism by enhancing  $Mg^{2+}$  block via activation of voltage independent potassium channels. *J. Neural Transm.* **1999**, *106*, 857–867.
- (95) Kornhuber, J.; Bormann, J.; Retz, W.; Hübers, M.; Riederer, P. Memantine displaces [ $^3H$ ]MK-801 at therapeutic concentrations in postmortem human frontal cortex. *Eur. J. Pharmacol.* **1989**, *166*, 589–590.
- (96) Kornhuber, J.; Bormann, J.; Hübers, M.; Rusche, K.; Riederer, P. Effects of the 1-amino-adamantanes at the MK-801-binding site of the NMDA-receptor-gated ion channel: A human postmortem brain study. *Eur. J. Pharmacol., Mol. Pharmacol. Sect.* **1991**, *206*, 297–300.
- (97) Gulbins, E.; Kolesnick, R. Measurement of sphingomyelinase activity. *Methods Enzymol.* **2000**, *322*, 382–388.
- (98) Armstrong, J.; Barlow, R. B. The ionization of phenolic amines, including apomorphine, dopamine and catecholamines and an assessment of zwitterion constants. *Br. J. Pharmacol.* **1976**, *57*, 501–516.
- (99) Mannhold, R.; Dross, K. P.; Rekker, R. F. Drug lipophilicity in QSAR practice: I. A comparison of experimental with calculative approaches. *Quant. Struct.-Act. Relat.* **1990**, *9*, 21–28.
- (100) Selassie, C. D.; Hansch, C.; Khwaja, T. A. Structure–activity relationships of antineoplastic agents in multidrug resistance. *J. Med. Chem.* **1990**, *33*, 1914–1919.
- (101) Krah, M. E.; Keltch, A. K.; Clowes, G. H. A. The role for changes in extracellular and intracellular hydrogen ion concentration in the action of local anesthetic bases. *J. Pharmacol. Exp. Ther.* **1940**, *68*, 330–350.
- (102) Slater, B.; McCormack, A.; Avdeef, A.; Comer, J. E. pH-metric log P. 4. Comparison of partition coefficients determined by HPLC and potentiometric methods to literature values. *J. Pharm. Sci.* **1994**, *83*, 1280–1283.
- (103) Scherman, D.; Gasnier, B.; Jaudon, P.; Henry, J.-P. Hydrophobicity of the tetrabenazine-binding site of the chromaffin granule monoamine transporter. *Mol. Pharmacol.* **1987**, *33*, 72–77.
- (104) Wan, H.; Holmen, A. G.; Wang, Y.; Lindberg, W.; Englund, M.; Nagard, M. B.; Thompson, R. A. High-throughput screening of  $pK_a$  values of pharmaceuticals by pressure-assisted capillary electrophoresis and mass spectrometry. *Rapid Commun. Mass Spectrom.* **2003**, *17*, 2639–2648.
- (105) Clarke, F. H.; Cahoon, N. M. Ionization constants by curve fitting: Determination of partition and distribution coefficients of acids and bases and their ions. *J. Pharm. Sci.* **1987**, *76*, 611–620.
- (106) Bosman, I. J.; Ensing, K.; de Zeeuw, R. A. Selection and evaluation of anticholinergics for transdermal drug delivery. *Int. J. Pharm.* **1998**, *169*, 75–82.
- (107) Schmid, J.; Koss, F. W. Assay of bromhexine in human plasma by capillary gas–liquid chromatography with nitrogen-selective detection and selected ion monitoring. *J. Chromatogr.* **1982**, *227*, 71–81.
- (108) Calpena, A. C.; Blanes, C.; Moreno, J.; Obach, R.; Domenech, J. A comparative in vitro study of transdermal absorption of antiemetics. *J. Pharm. Sci.* **1994**, *83*, 29–33.
- (109) Belsner, K.; Pfeifer, M.; Wilffert, B. Reversed-phase high-performance liquid chromatography for evaluating the lipophilicity of pharmaceutical substances with ionization up to  $\log P_{app} = 8$ . *J. Chromatogr.* **1993**, *629*, 123–134.
- (110) Mach, R. H.; Elder, S. T.; Morton, T. E.; Nowak, P. A.; Evora, P. H.; Scripko, J. G.; Luedtke, R. R.; Unsworth, C. D.; Filtz, T.; Rao, A. V.; Molinoff, P. B.; Ehrenkaufer, R. L. E. The use of [ $^{18}F$ ]4-fluorobenzyl iodide (FBI) in PET radiotracer synthesis: Model alkylation studies and its application in the design of dopamine  $D_1$  and  $D_2$  receptor-based imaging agents. *Nucl. Med. Biol.* **1993**, *20*, 777–794.
- (111) Kaufman, J. J.; Koski, W. S.; Benson, D. N.; Semo, N. M. Narcotic and narcotic antagonist  $pK_a$ 's and partition coefficients and their significance in clinical practice. *Drug Alcohol Depend.* **1975**, *1*, 103–114.
- (112) Clarke, F. H. Ionization constants by curve fitting: Application to the determination of partition coefficients. *J. Pharm. Sci.* **1984**, *73*, 226–230.
- (113) El Tayar, N.; Kilpatrick, G. J.; van de Waterbeemd, H.; Testa, B.; Jenner, P.; Marsden, C. D. Interaction of neuroleptic drugs with rat striatal D-1 and D-2 dopamine receptors: A quantitative structure–affinity relationship study. *Eur. J. Med. Chem.* **1988**, *23*, 173–182.
- (114) Douglas, K. T.; Sharma, R. K.; Walmsley, J. F.; Hider, R. C. Ionization processes of some harmala alkaloids. *Mol. Pharmacol.* **1983**, *23*, 614–618.
- (115) ter Laak, A. M.; Tsai, R. S.; Donné-Op den Kelder, G. M.; Carrupt, P.-A.; Testa, B.; Timmerman, H. Lipophilicity and hydrogen-bonding

- capacity of H1-antihistaminic agents in relation to their central sedative side-effects. *Eur. J. Pharm. Sci.* **1994**, 2, 373–384.
- (116) Takás-Novák, K.; Avdeef, A. Interlaboratory study of log *P* determination by shake-flask and potentiometric methods. *J. Pharm. Biomed. Anal.* **1996**, 14, 1405–1413.
- (117) Seiler, P. The simultaneous determination of partition coefficient and acidity constant of a substance. *Eur. J. Med. Chem.* **1974**, 9, 663–665.
- (118) Ullrich, K. J.; Rumrich, G.; David, C.; Fritzsche, G. Bisubstrates: Substances that interact with renal contraluminal organic anion and organic cation transport systems. I. Amines, piperidines, piperazines, azepines, pyridines, quinolines, imidazoles, thiazoles, guanidines and hydrazines. *Pfluegers Arch.* **1993**, 425, 280–299.
- (119) Hafkenschied, T. L.; Tomlinson, E. Relationships between hydrophobic (lipophilic) properties of bases and their retention in reversed-phase liquid chromatography using aqueous methanol mobile phases. *J. Chromatogr.* **1984**, 292, 305–317.
- (120) Ishihama, Y.; Nakamura, M.; Miwa, T.; Kajima, T.; Asakawa, N. A rapid method for *pK<sub>a</sub>* determination of drugs using pressure-assisted capillary electrophoresis with photodiode array detection in drug discovery. *J. Pharm. Sci.* **2002**, 91, 933–942.
- (121) Franke, U.; Munk, A.; Wiese, M. Ionization constants and distribution coefficients of phenothiazines and calcium channel antagonists determined by a pH-metric method and correlation with calculated partition coefficients. *J. Pharm. Sci.* **1999**, 88, 89–95.
- (122) *The Merck Index—An encyclopedia of chemicals, drugs, and biologicals*; Merck Research Laboratories Division of Merck & Co., Inc.: Whitehouse Station, NJ, 2006.
- (123) SRC PhysProp Database. [www.syrres.com/esc/physdemo.htm](http://www.syrres.com/esc/physdemo.htm) (2007) Syracuse Research Corporation.
- (124) Henkel, J. G.; Hane, J. T. Structure-anti-Parkinson activity relationships in the aminoadamantanes. Influence of bridgehead substitution. *J. Med. Chem.* **1982**, 25, 51–56.
- (125) Brodin, A. Rates of transfer of organic protolytic solutes between an aqueous and an organic phase. 3. Mass transfer between water and some polar organic liquids. *Acta Pharm. Suec.* **1974**, 11, 141–148.
- (126) Boudier, H. S.; de Boer, J.; Smeets, G.; Lien, E. J.; van Rossum, J. Structure activity relationships for central and peripheral alpha adrenergic activities of imidazoline derivatives. *Life Sci.* **1975**, 17, 377–385.

JM070524A